97

SATELLITE & MESOMETEOROLOGY RESEARCH PROJECT

Department of the Geophysical Sciences
The University of Chicago

TORNADO OCCURRENCES RELATED TO OVERSHOOTING CLOUD-TOP HEIGHTS AS DETERMINED FROM ATS PICTURES

by

T. Theodore Fujita

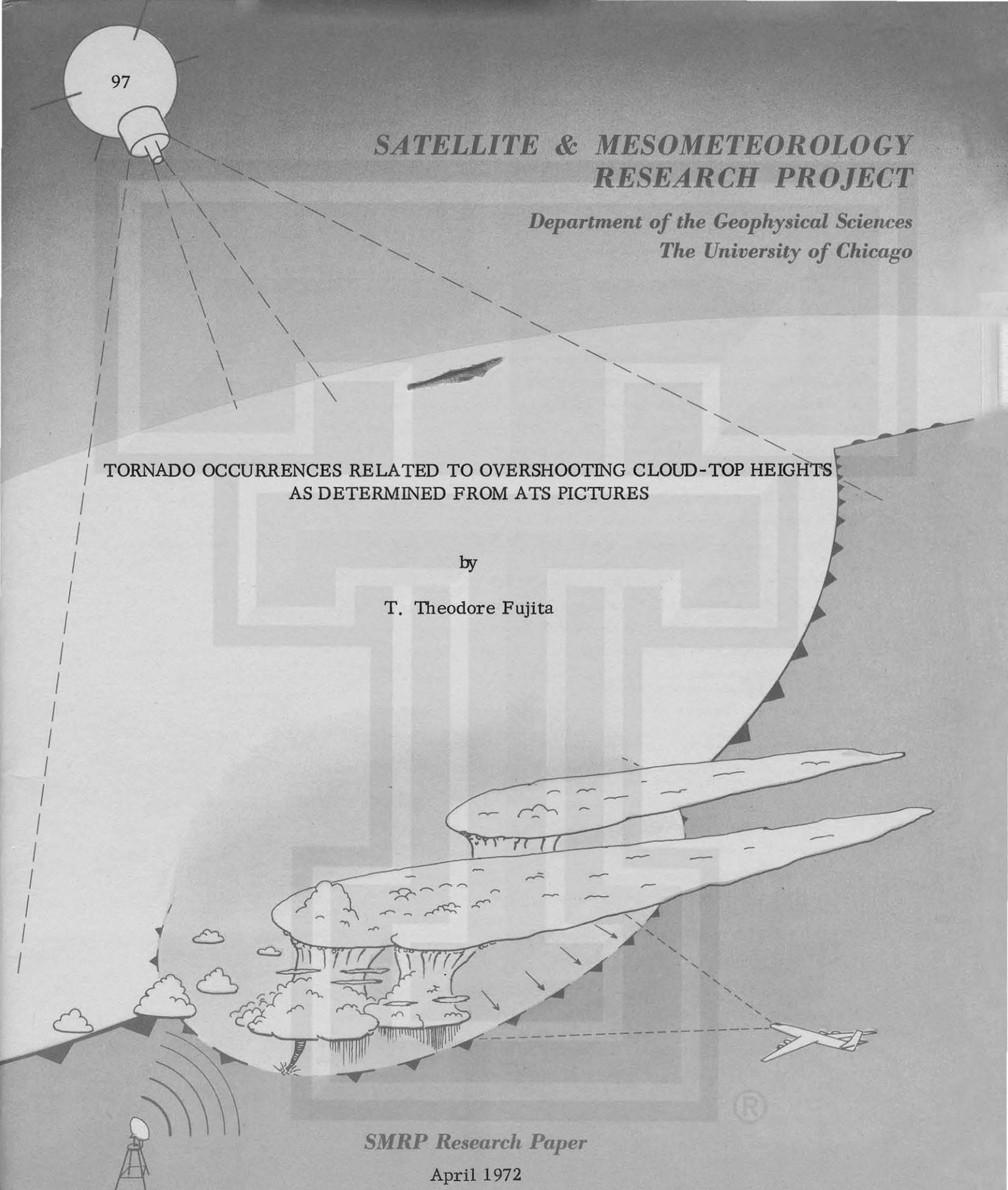

SMRP Research Paper

April 1972

MESOMETEOROLOGY PROJECT --- RESEARCH PAPERS

1.* Report on the Chicago Tornado of March 4, 1961 - Rodger A. Brown and Tetsuya Fujita

2.* Index to the NSSP Surface Network - Tetsuya Fujita

3.* Outline of a Technique for Precise Rectification of Satellite Cloud Photographs - Tetsuya Fujita

4.* Horizontal Structure of Mountain Winds - Henry A. Brown

5.* An Investigation of Developmental Processes of the Wake Depression Through Excess Pressure Analysis of Nocturnal Showers - Joseph L. Goldman

6.* Precipitation in the 1960 Flagstaff Mesometeorological Network - Kenneth A. Styber

7.** On a Method of Single- and Dual-Image Photogrammetry of Panoramic Aerial Photographs - Tetsuya Fujita

8. A Review of Researches on Analytical Mesometeorology - Tetsuya Fujita

9.* Meteorological Interpretations of Convective Nephsystems Appearing in TIROS Cloud Photographs - Tetsuya Fujita, Toshimitsu Ushijima, William A. Hass, and George T. Dellert, Jr.

10.* Study of the Development of Prefrontal Squall-Systems Using NSSP Network Data - Joseph L. Goldman

11. Analysis of Selected Aircraft Data from NSSP Operation, 1962 - Tetsuya Fujita

12. Study of a Long Condensation Trail Photographed by TIROS I - Toshimitsu Ushijima

13. A Technique for Precise Analysis of Satellite Data; Volume I - Photogrammetry (Published as MSL Report No. 14) - Tetsuya Fujita

14. Investigation of a Summer Jet Stream Using TIROS and Aerological Data - Kozo Ninomiya

15. Outline of a Theory and Examples for Precise Analysis of Satellite Radiation Data - Tetsuya Fujita

16. Preliminary Result of Analysis of the Cumulonimbus Cloud of April 21, 1961 - Tetsuya Fujita and James Arnold

17. A Technique for Precise Analysis of Satellite Photographs - Tetsuya Fujita

18.* Evaluation of Limb Darkening from TIROS III Radiation Data - S.H.H. Larsen, Tetsuya Fujita, and W.L. Fletcher

19. Synoptic Interpretation of TIROS III Measurements of Infrared Radiation - Finn Pedersen and Tetsuya Fujita

20.* TIROS III Measurements of Terrestrial Radiation and Reflected and Scattered Solar Radiation - S.H.H. Larsen, Tetsuya Fujita, and W.L. Fletcher

21. On the Low-level Structure of a Squall Line - Henry A. Brown

22.* Thunderstorms and the Low-level Jet - William D. Bonner

23.* The Mesoanalysis of an Organized Convective System - Henry A. Brown

24. Preliminary Radar and Photogrammetric Study of the Illinois Tornadoes of April 17 and 22, 1963 - Joseph L. Goldman and Tetsuya Fujita

25. Use of TIROS Pictures for Studies of the Internal Structure of Tropical Storms - Tetsuya Fujita with Rectified Pictures from TIROS I Orbit 125, R/O 128 - Toshimitsu Ushijima

26. An Experiment in the Determination of Geostrophic and Isallobaric Winds from NSSP Pressure Data - William Bonner

27. Proposed Mechanism of Hook Echo Formation - Tetsuya Fujita with a Preliminary Mesosynoptic Analysis of Tornado Cyclone Case of May 26, 1963 - Tetsuya Fujita and Robbi Stuhmer

28. The Decaying Stage of Hurricane Anna of July 1961 as Portrayed by TIROS Cloud Photographs and Infrared Radiation from the Top of the Storm - Tetsuya Fujita and James Arnold

29. A Technique for Precise Analysis of Satellite Data, Volume II - Radiation Analysis, Section 6. Fixed-Position Scanning - Tetsuya Fujita

30. Evaluation of Errors in the Graphical Rectification of Satellite Photographs - Tetsuya Fujita

31. Tables of Scan Nadir and Horizontal Angles - William D. Bonner

32. A Simplified Grid Technique for Determining Scan Lines Generated by the TIROS Scanning Radiometer - James E. Arnold

33. A Study of Cumulus Clouds over the Flagstaff Research Network with the Use of U-2 Photographs - Dorothy L. Bradbury and Tetsuya Fujita

34. The Scanning Printer and Its Application to Detailed Analysis of Satellite Radiation Data - Tetsuya Fujita

35. Synoptic Study of Cold Air Outbreak over the Mediterranean using Satellite Photographs and Radiation Data - Aasmund Rabbe and Tetsuya Fujita

36. Accurate Calibration of Doppler Winds for their use in the Computation of Mesoscale Wind Fields - Tetsuya Fujita

37. Proposed Operation of Intrumented Aircraft for Research on Moisture Fronts and Wake Depressions - Tetsuya Fujita and Dorothy L. Bradbury

38. Statistical and Kinematical Properties of the Low-level Jet Stream - William D. Bonner

39. The Illinois Tornadoes of 17 and 22 April 1963 - Joseph L. Goldman

40. Resolution of the Nimbus High Resolution Infrared Radiometer - Tetsuya Fujita and William R. Bandeen

41. On the Determination of the Exchange Coefficients in Convective Clouds - Rodger A. Brown

* Out of Print
** To be published

(Continued on back cover)

TORNADO OCCURRENCES RELATED TO OVERSHOOTING CLOUD-TOP HEIGHTS AS DETERMINED FROM ATS PICTURES

by

T. Theodore Fujita
Department of Geophysical Sciences
The University of Chicago

SMRP Research Paper 97
April 1972

The research reported in this paper has been sponsored by NASA under grant NGR 14-001-008 and by NOAA (MSL) under grant E-198-68 (G).

Tornado Occurrences related to Overshooting Cloud-Top Heights as determined from ATS Pictures

T. Theodore Fujita

Abstract

A sequence of ATS III pictures including the development history of large anvil clouds near Salina, Kansas was enlarged by NASA into 8X negatives which were used to obtain the best quality prints by mixing scan lines in 8 steps to minimize checker-board patterns. These images resulted in the best possible resolution, permitting us to compute the heights of overshooting tops above environmental anvil levels based on cloud shadow relationships along with the techniques of lunar topographic mapping. Of 39 heights computed, 6 were within 15 miles of reported positions of 3 tornadoes. It was found that the tornado proximity tops were mostly less than 5000 ft, with one exception of 7,000 ft, suggesting that tornadoes are most likely to occur when overshooting height decreases.

In order to simulate surface vortices induced by cloud-scale rotation and updraft fields, a laboratory model was constructed. The model experiment has shown that the rotation or updraft field induces a surface vortex but their combination does prevent the formation of the surface vortex. This research leads to a conclusion that the determination of the cloud-top topography and its time variation is of extreme importance in predicting severe local storms for a period of 0 to 6 hours.

1. INTRODUCTION

Typical anvil clouds grow from the tops of tall convective clouds reaching or penetrating the tropopause where the combination of stable lapse rate and strong winds tend to spread hydrometeors in horizontal directions. Although an anvil spreading from an intense cell often grows upwind, its rapid growth toward the relative downwind direction is commonly observed in ATS picture sequences.

Hydrometeors are transported upward inside strong updrafts which tend to overshoot beyond the crossover point at which the indraft and environmental temperatures coincide. The height of the crossover point does not always coincide with that of the tropopause because the vertical distributions of the indraft and the environmental temperatures do result in the variation of the crossover point on both sides of the tropopause level.

The air parcel rising through the crossover point is characterized by the neutral bouyancy as well as the vertical component of large momentum of indraft air. A process of "overshooting" takes place until the rising air reaches an equilibirium at some altitude above the crossover point, where the updraft parcels cease to rise. A dome protruding beyond the level of overall anvil will appear over the top of an overshooting updraft. Such a dome is called either "protruding top" or "overshooting top".

Terrestrial photogrammetric analyses of Alberta hailstorms by Renick (1971) revealed the time variation of cloud-tower tops overshooting up to 3 km (10,000 ft) above the tropopause located at 12.6 km (41,000 ft) MSL. Some tower tops had a maximum rate of rise of 20 m sec^{-1} at the tropopause beyond which the rate decreased gradually. This study also revealed that the time between the tropopause crossing and the highest growth point of a tower top is only about 3 min. Shortly after reaching its highest growth point, each top subsided rather gradually. These evidences clearly indicate the rate of change in the overshooting height and its maximum height are closely related to the vertical motions taking place beneath the anvil cloud.

Occurrences of both hailstorms and tornadoes are to be related to the heights of cloud tops. Despite such expectation, Lee (1971) found that the dome protrusion of 29 cases of tornado-producing thunderstorms varies from just above the level of the cirrus to 2.5 km (8,000 ft) above the cirrus, with a mean of 0.6 km (2,000 ft). These heights were computed from RB-57F pictures taken by horizon-to-horizon camera. 471 cases of thunderstorm tops over Oklahoma showed much larger variations in cloud-top heights with 1% probability for height range, 18.0 km (59,000 ft) or

higher; 4%, 17.0 km (56,000 ft) - 17.9 km; 10%, 16.0 km (52,000 ft) - 16.9 km, etc. Based on these results Lee concluded that he could not find practical means for identifying tornado-producing thunderstorms from RB-57F traverses and subsequent photogrammetric computation.

Bonner and Kemper (1971) reached a similar but slightly different conclusion through their statistical study of echo-top heights over the central, eastern, and southern U.S., in relation to tornado and hailstorm occurrences. Over the central U.S., according to their statistics, both tornado and hail probabilities increase significantly when echo-top heights exceed the tropopause. Thereafter hail probability increases very rapidly with the echo-top height while tornado probability shows only a slight increase. This evidence implies that tornado occurrences are closely related to the tropopause penetration of echo tops but not to their excessive height above the tropopause.

Tornado-producing thunderstorms are, thus, very unlikely to be characterized by excessive height of overshooting tops, at least during the stage of tornado formation. It would be important, therefore, to investigate the time variation of the cloud-top topography of tornado-producing thunderstorms during their entire life history.

2. ANVIL-TOP TOPOGRAPHY

A detailed view of a thunderstorm with a circular anvil is presented in Fig. 1. The picture was taken from Apollo 9 while orbiting over Columbia on March 8, 1969. The diameter of the anvil was 75 km (45 mi), characterized by an isolated overshooting top near the center of the anvil. The overshooting height above the environmental anvil can be computed from a 30° elevation angle of the sun at 1645 Local Standard Time when this picture was taken. The overshooting height, thus obtained, was 4.3 km (14,000 ft) with a 7.5 km (4.7 mi) diameter of the protrusion dome. The anvil top around the overshooting top is not flat like a table top, instead a bumpy feature implies the past history of the thunderstorm activities.

Growth of towering cumuli into anvil clouds takes place rather rapidly. As shown in Renick's (1971) hailstorm cases, a 20 m sec^{-1}, growth rate will increase the cloud-top height at the rate of 1.2 km min^{-1}, thus requiring only about 10 min to reach the tropopause. A series of side views of fast-growing towering Cu - Cb

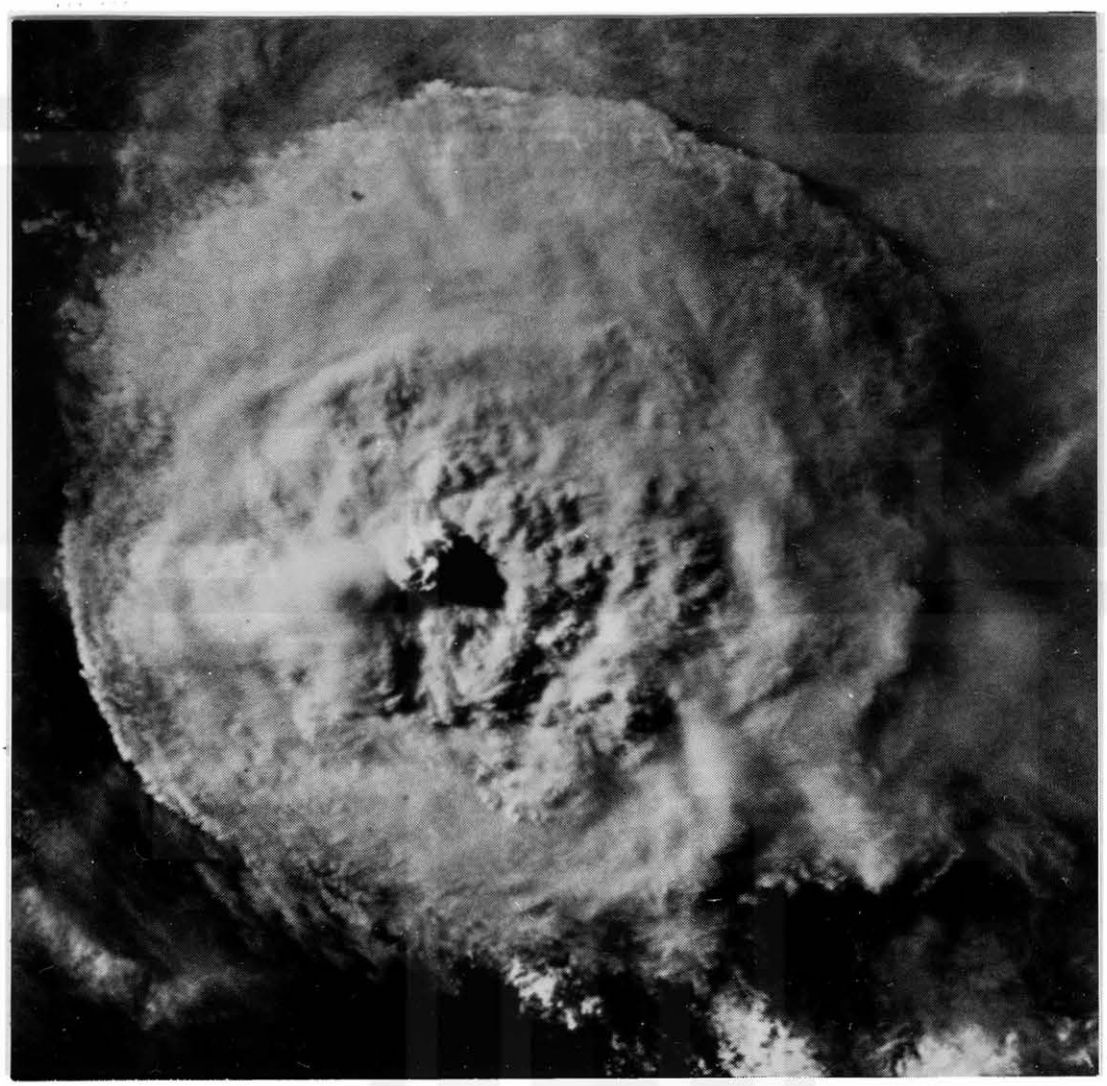

Fig. 1. Apollo 9 photograph of an anvil top over Colombia, South America, March 8, 1969

of April 21, 1961 as reported by Fujita and Arnold (1963) is reproduced in Fig. 2. The sequence was made from 16mm movie taken by a nose camera of RFF B-57 aircraft. It is seen that both clouds B and D grew from Cu to Cb in 10 to 15 min., suggesting that 3 to 5-min picture intervals are required for the purpose of investigating the growth mechanism of such clouds. These clouds developed into a rotating thunderstorm at 1749 CST, a picture of which was used as cover photograph of Bulletin of AMS, April 1965. A tornado from this cloud between 1800 and 1805 left a 6-mile damage swath in eastern Kansas. The time between the towering Cu

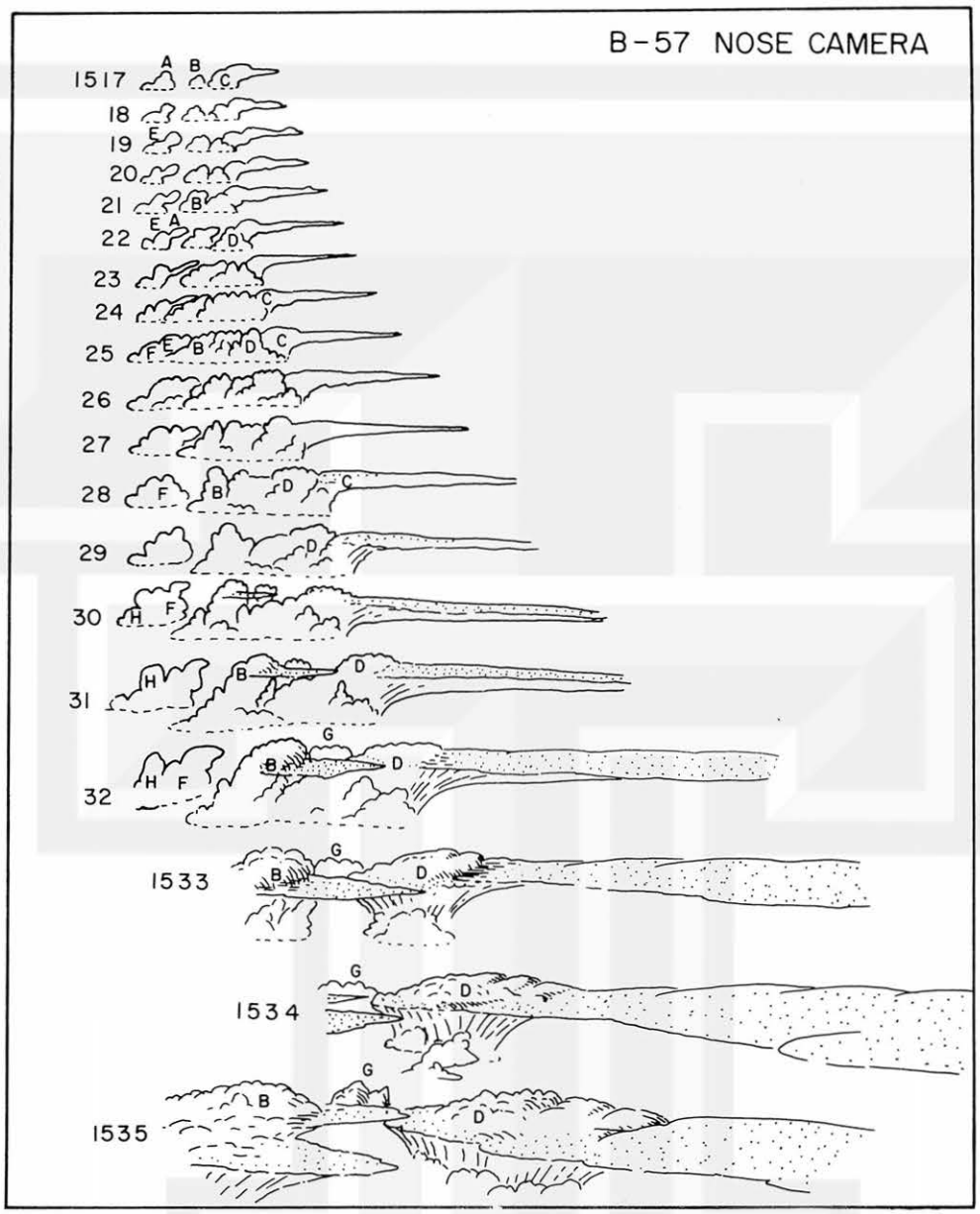

Fig. 2. View of growing anvils of April 21, 1961. This one-minute sequence was drawn based on the time-lapse film taken by the nose camera of a B-57. Distance to the cloud varied from 150 miles to about 10 miles.

stage, 1517 CST in Fig. 2 and the tornado touchdown at 1800 was 2 hr. and 43 min., suggesting that a continuous surveillance of the anvil-top topography is useful in understanding and predicting the behavior of tornado-producing thunderstorms.

One of the best sequence of ATS III pictures showing time changes in the anvil-top topography was obtained by mixing lines of 8X enlargement pictures

produced by the Goddard Space Flight Center. Original 8X pictures are of wide scan bands, each of which was produced by repeating eight lines modulated by 4096 picture element pulses. Due to these eight repetitions, image elements appear to elongate vertically into rectangles with 2:1 side ratio, because the left-right picture-element pulses of 4096 are almost twice in number of the 2400 scan lines. In order to create a smoothed image by suppressing distinct scan bands, line-mixed images were produced simply by exposing a photographic paper eight times while shifting the paper as much as one scan-line distance after each exposure.

Presented in Fig. 3 are ATS III pictures of anvil clouds of May 11-12, 1970 near Salina, Kansas. These pictures, taken every 11 minutes, were gridded with 0.5 deg. longitudes and latitudes. During the picture sequence period of 2 hr 01 min, the solar elevation angle decreased from 30° to 8° at the anvils' location. Corresponding to this solar elevation angle the distance between the cloud and shadow points on the earth increased significantly from 2.6 to 8.2 times the cloud height. This means that the cloud height resolution increases several times when computed from the cloud-shadow distance. Various quantities were computed by rectifying each picture into a plan view with approximate cloud-top relief as shown in Figs. 4 - 15. The figure includes PP1 echoes from Wichita, Kansas (ICT) and Kansas City, Missouri (MKC) as well as their boundaries drawn in the rectified cloud map. The heights of overshooting tops above environmental anvil surface are given in feet, such as 2000, 4000, etc.

At 2224, two small echoes, only a few miles across, are seen in the Wichita radar picture while corresponding clouds in the ATS picture covered 900 and 1,100 sq. km. By 2307 a bird-shaped echo developed near the center of the fast-growing anvil area covering 3.800 sq. km. There was no distinct shadow corresponding to the bird-shaped echo, while the small echo to the southwest was characterized by a distinct shadow. A tornado, 2320-25, touched down briefly near Westfall from the small echo while the bird-shaped echo, still maintaining its identity, produced no tornadoes. Thereafter the small echo started growing rapidly both in area and intensity, meanwhile the bird-shaped echo disintegrated gradually.

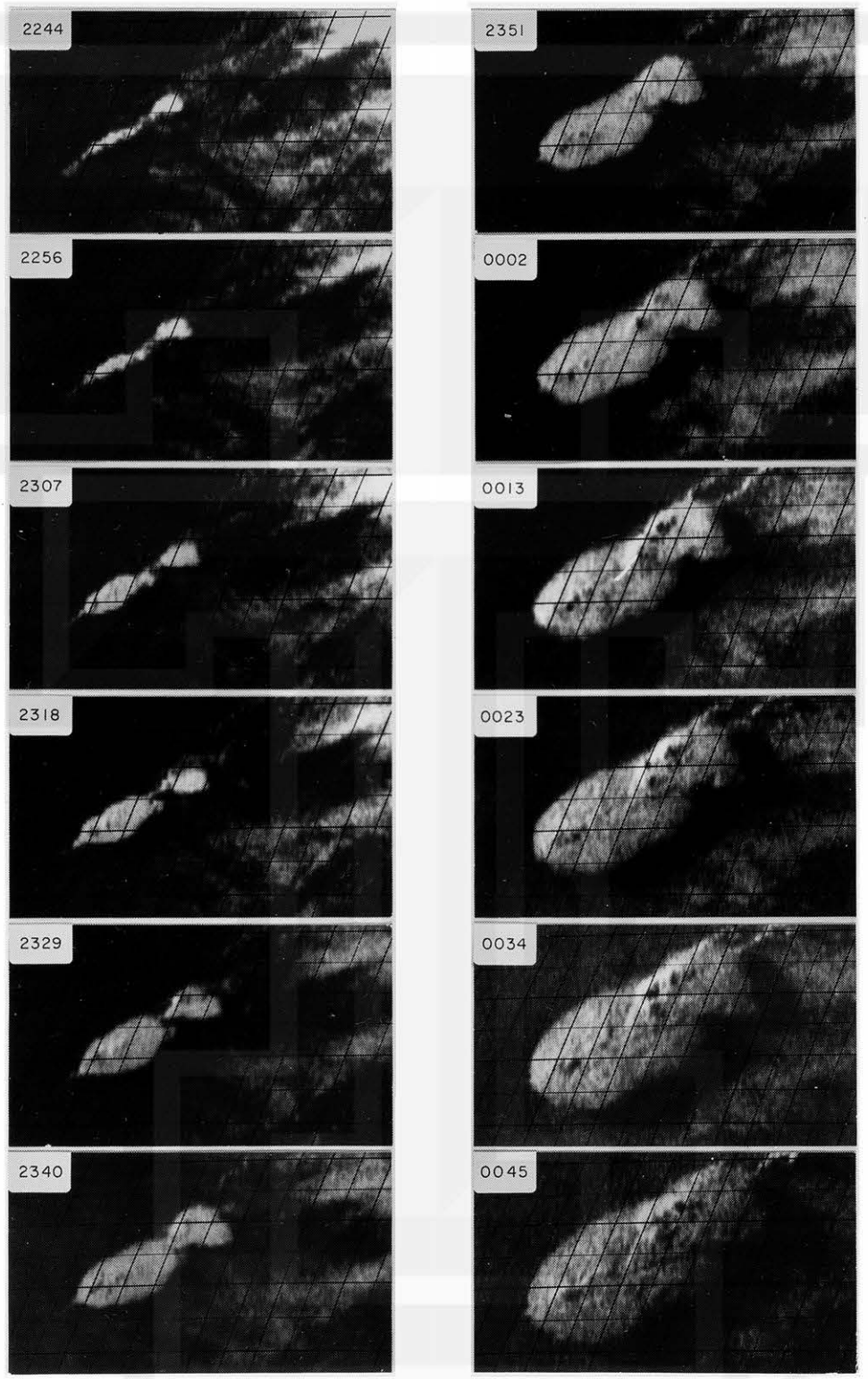

Fig. 3. ATS III view of growing anvils near Salina, Kansas. These 11-minute interval pictures were taken between 2244 Z, May 11 and 0045 Z, May 12, 1970.

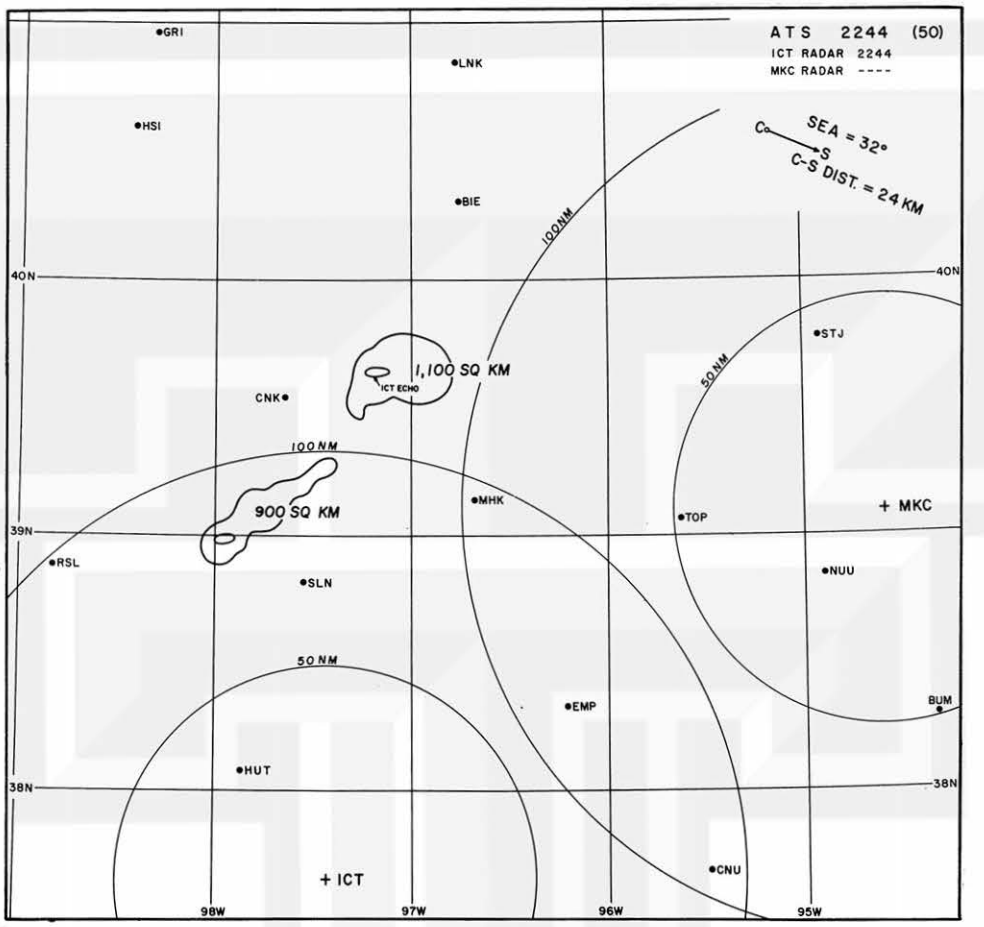

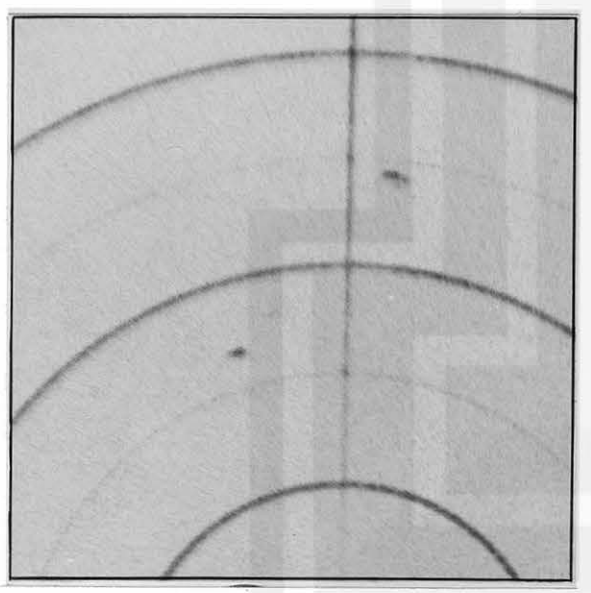

NO PICTURE AVAILABLE

Fig. 4. ATS cloud patterns at 2244 GMT, May 11, 1970 and radar pictures from Wichita (left). Kansas City radar was not taking pictures because the clouds were too far from the station.

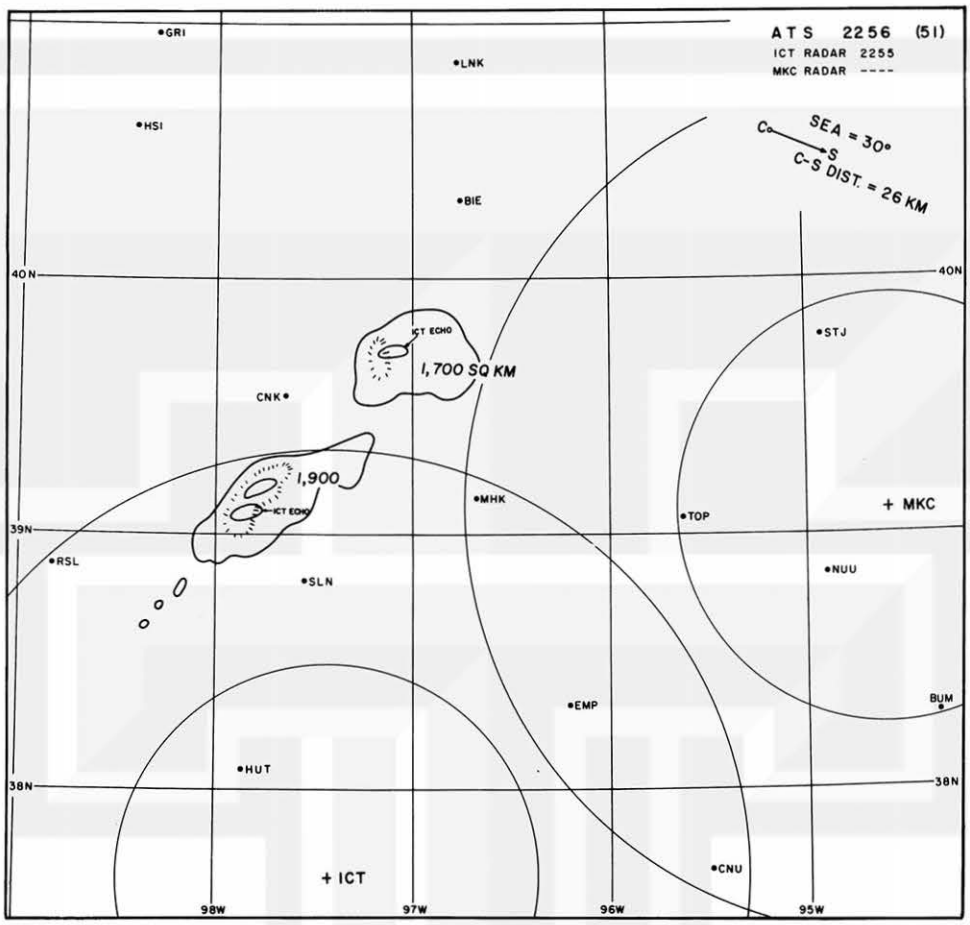

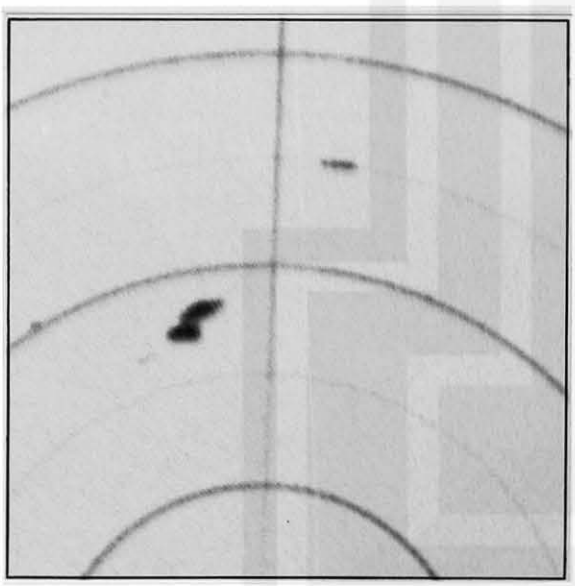

NO PICTURE AVAILABLE

Fig. 5. ATS cloud patterns at 2256 GMT, May 11, 1970 and radar pictures from Wichita (left). Three small echoes were seen from Wichita.

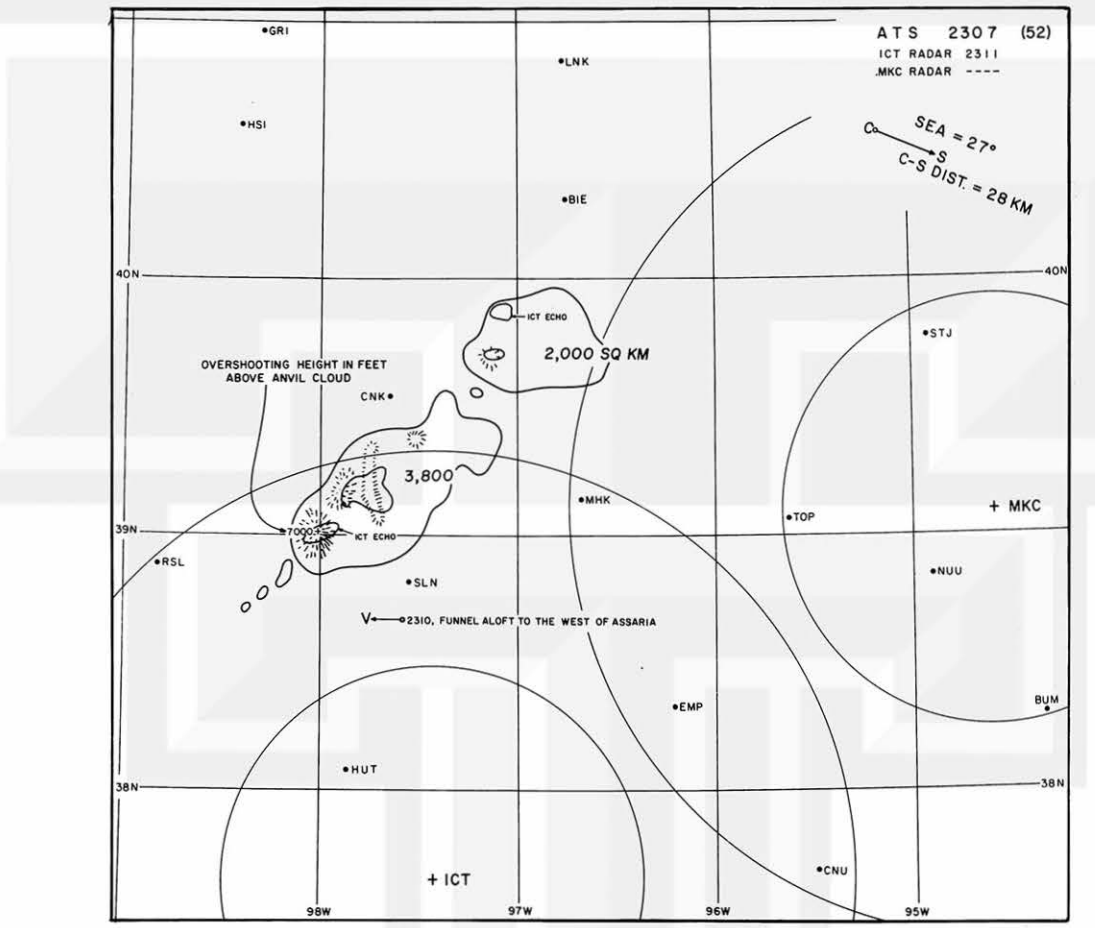

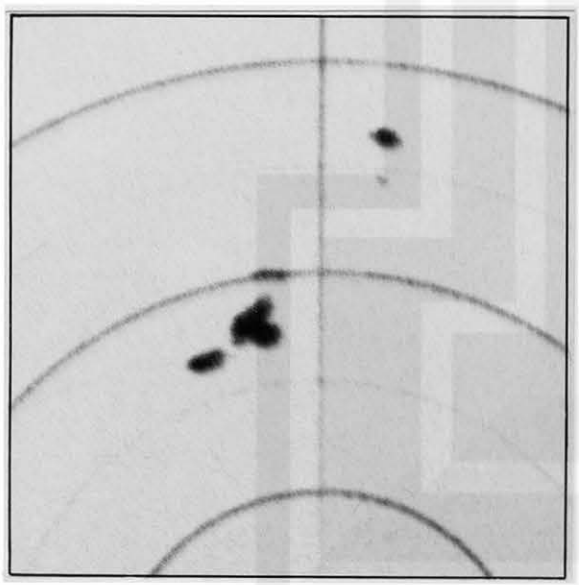

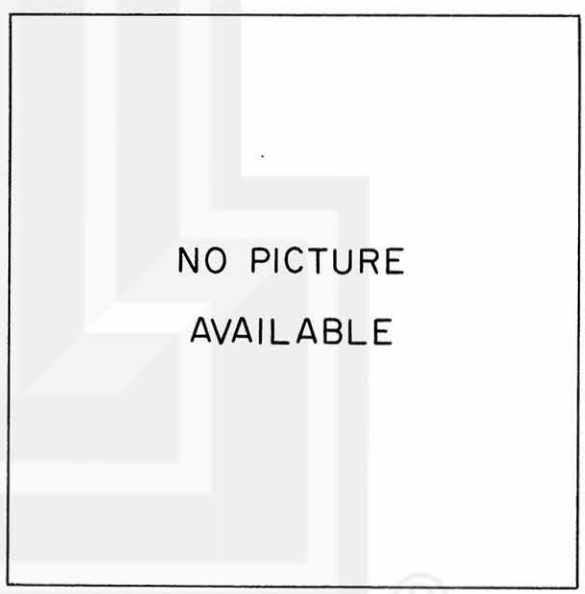

Fig. 6. ATS cloud patterns at 2307 GMT, May 11, 1970 and radar pictures from Wichita (left). A report of funnel cloud to the west of Assaria must be an error either in time or location.

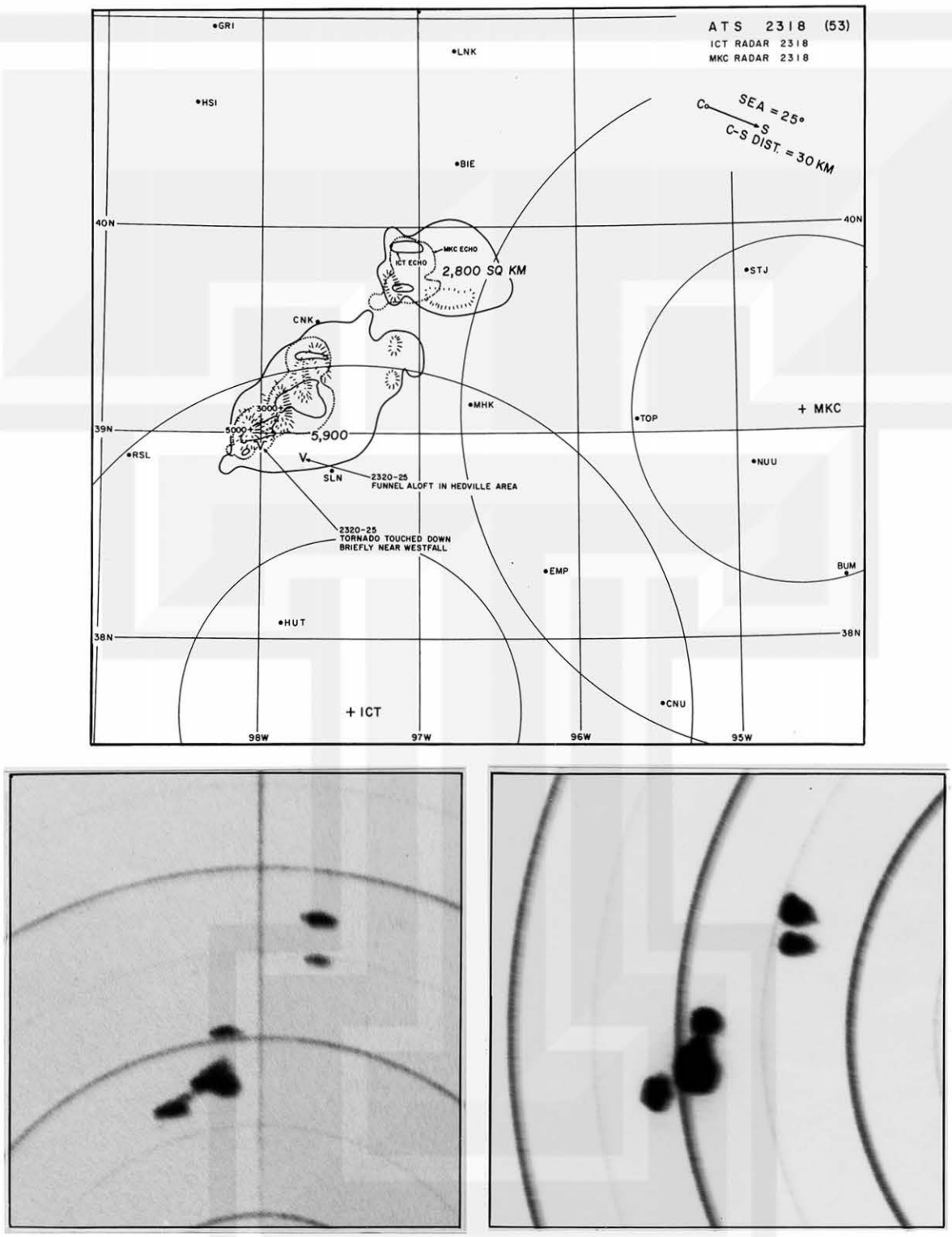

Fig. 7. ATS cloud patterns at 2318 GMT, May 11, 1970 and radar pictures from Wichita (left) and Kansas City, Missouri.

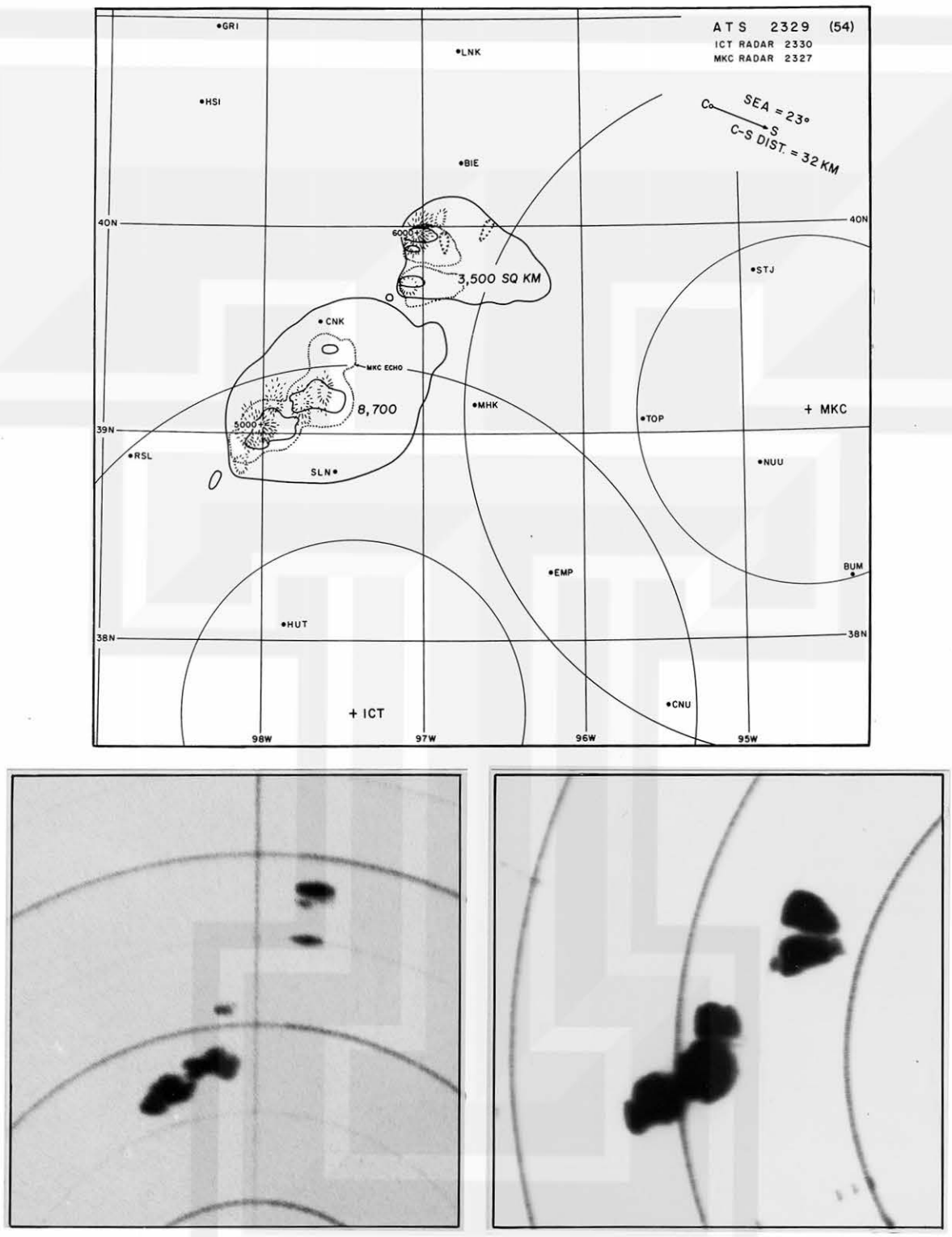

Fig. 8. ATS cloud patterns at 2329 GMT, May 11, 1970 and radar pictures from Wichita (left) and Kansas City, Missouri.

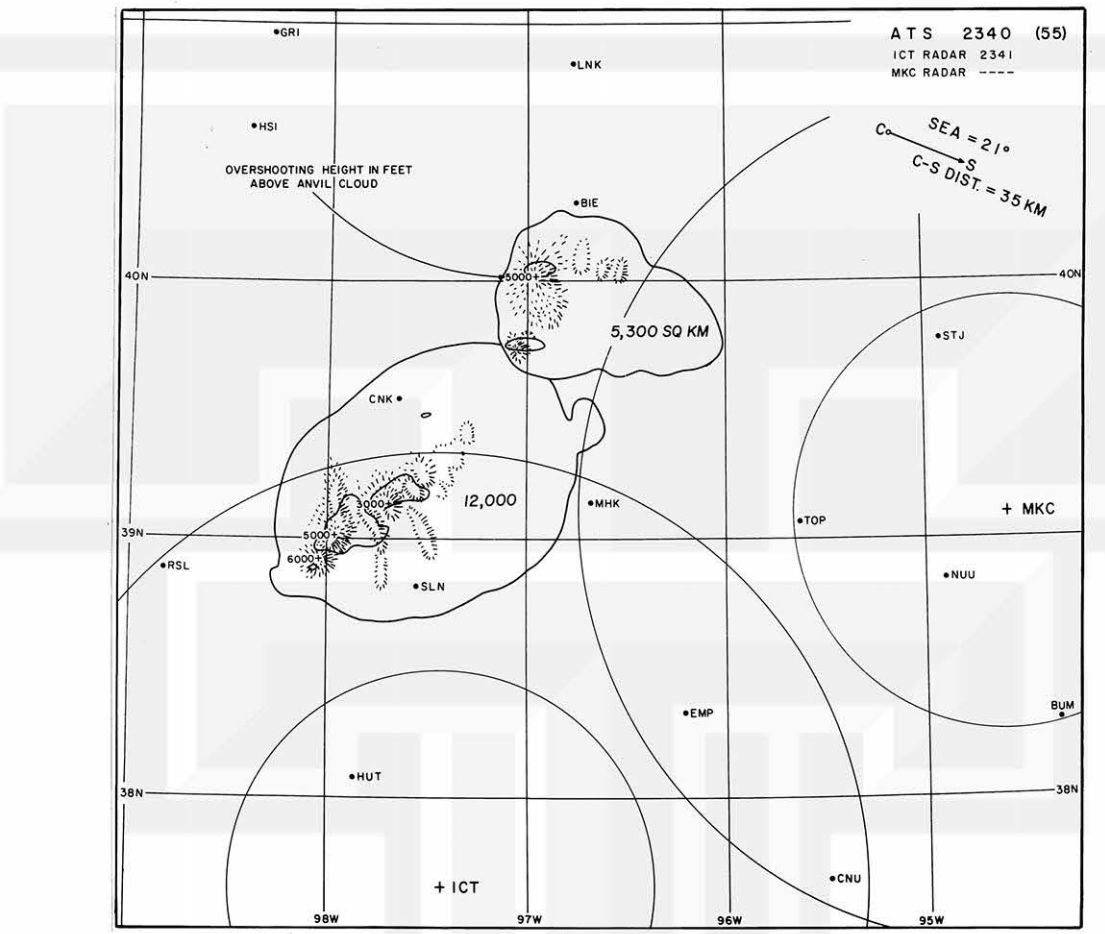

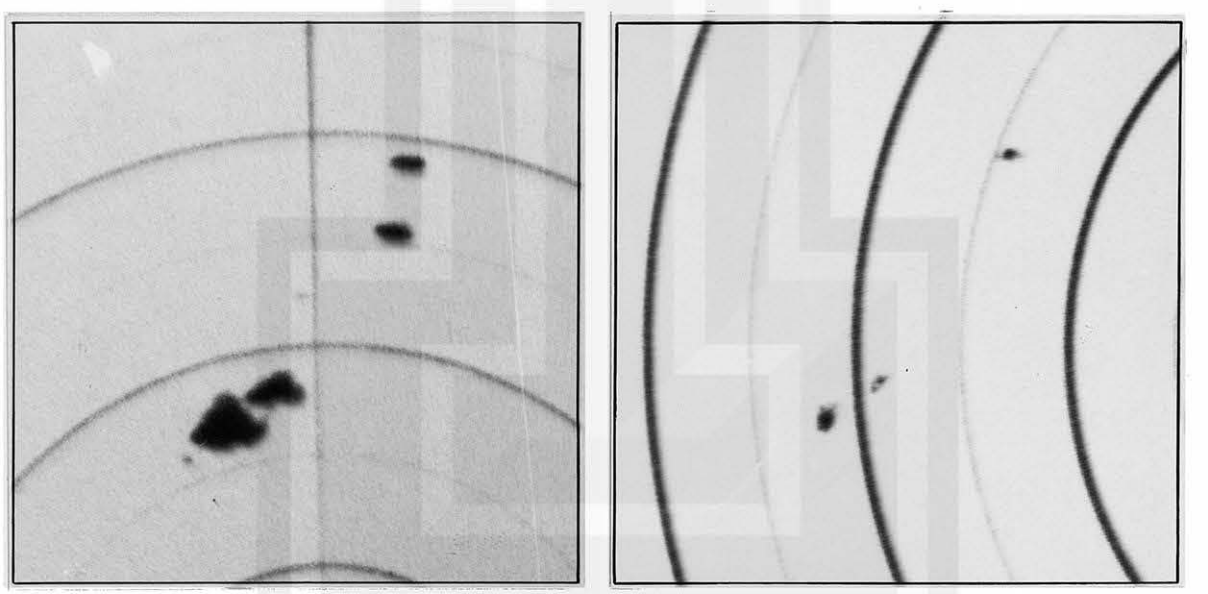

Fig. 9. ATS cloud patterns at 2340 GMT, May 11, 1970 and radar pictures from Wichita (left) and Kansas City, Missouri. Gain of Kansas City radar was reduced.

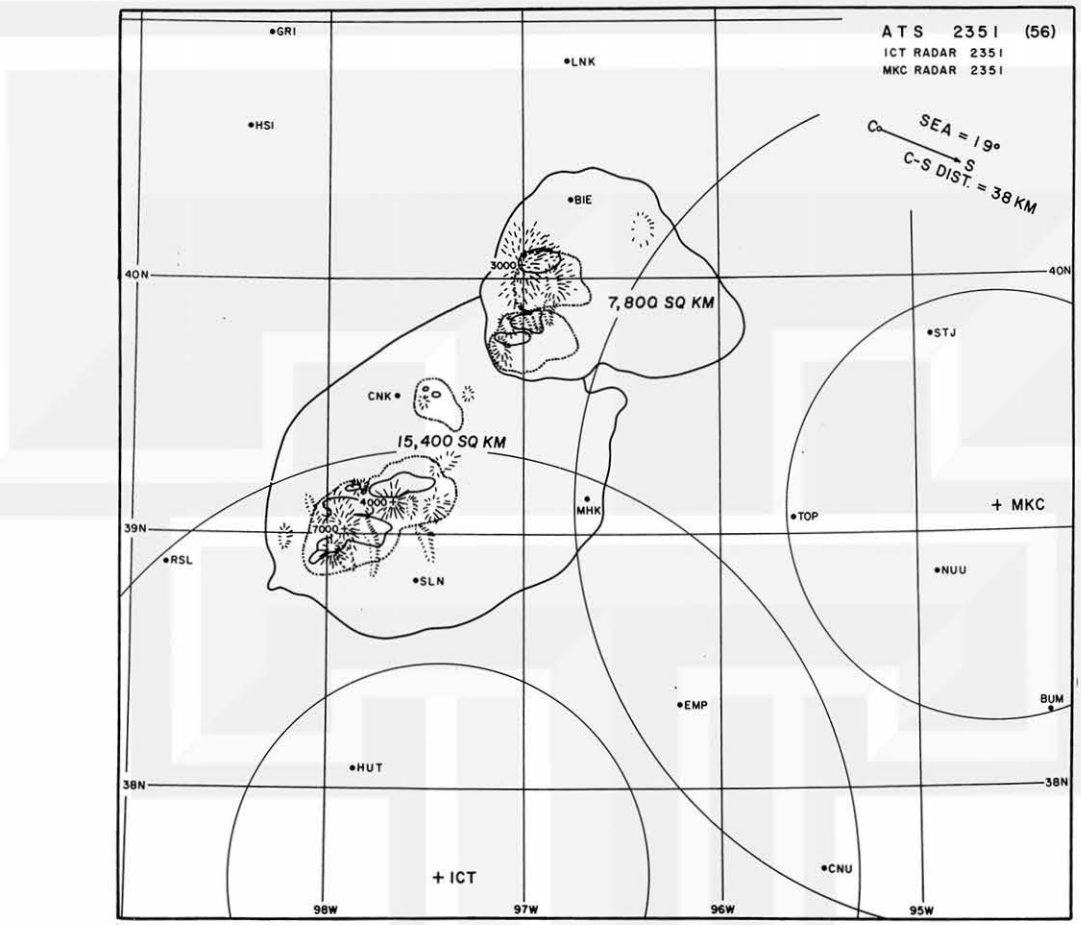

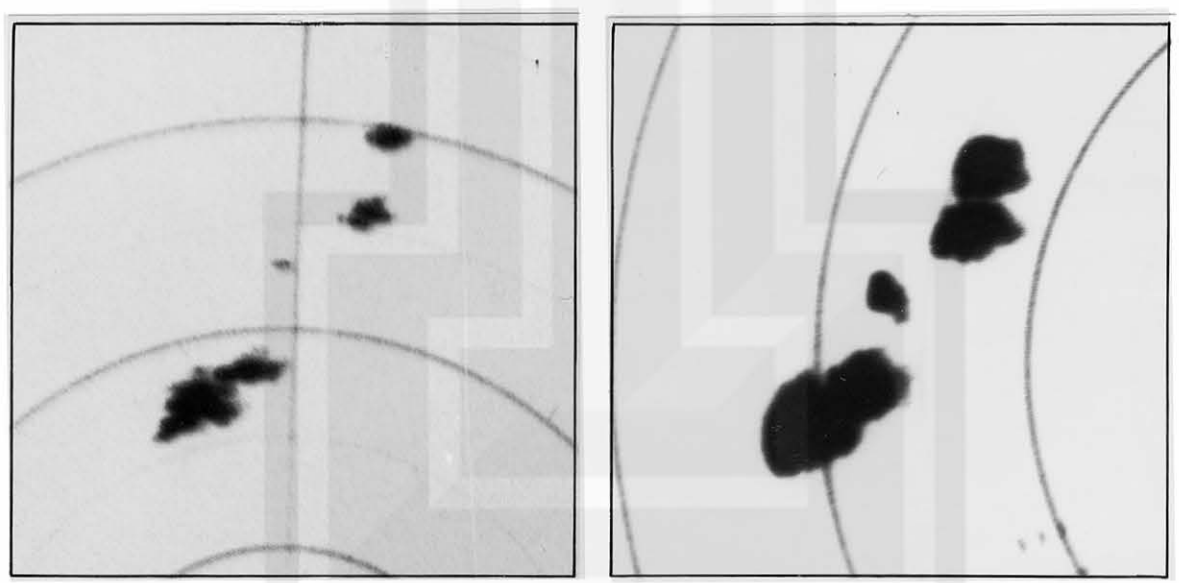

Fig. 10. ATS cloud patterns at 2351 GMT, May 11, 1970 and radar pictures from Wichita (left) and Kansas City, Missouri.

Fig. 11. ATS cloud patterns at 0002 GMT, May 12, 1970 and radar pictures from Wichita (left) and Kansas City, Missouri.

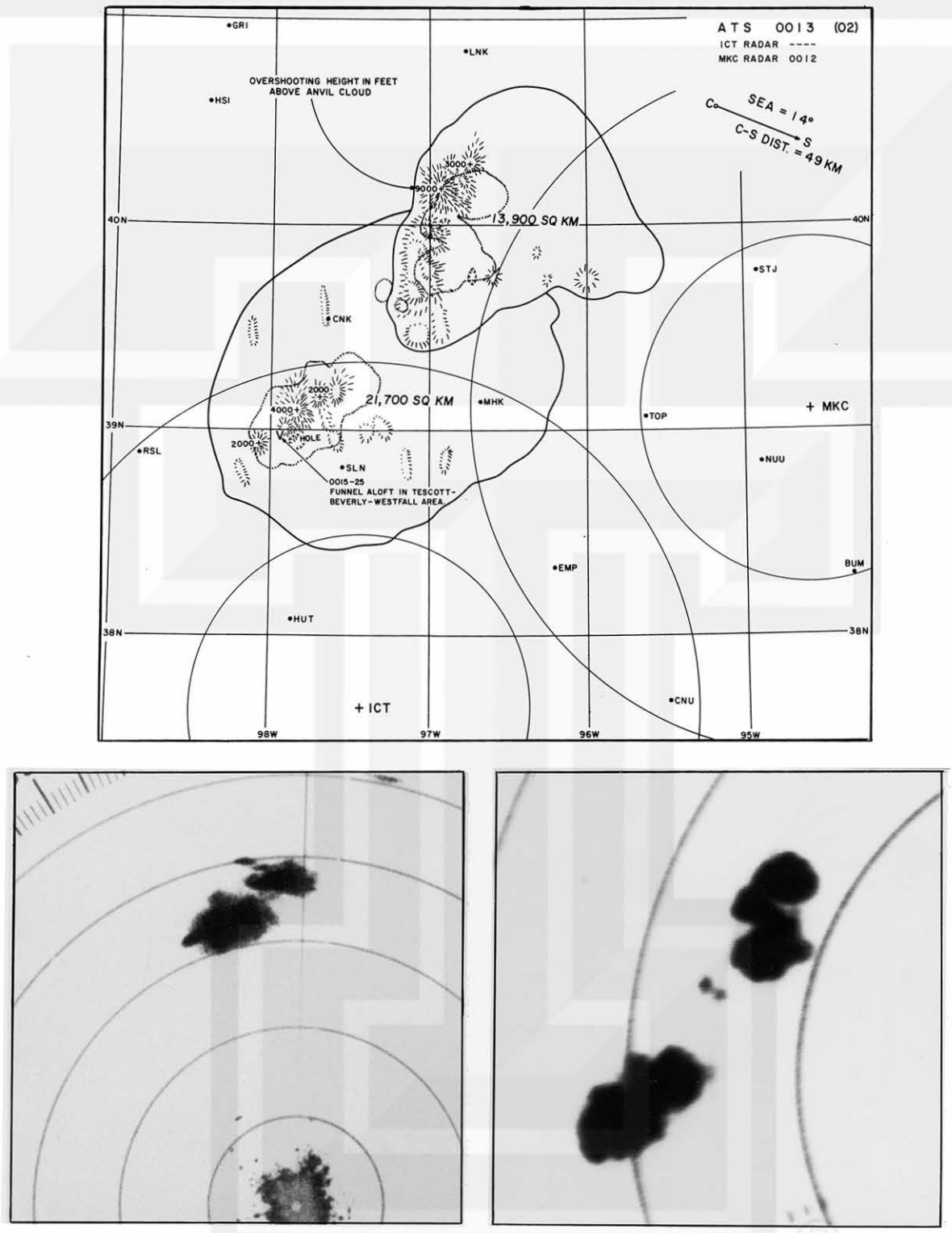

Fig. 12. ATS cloud patterns at 0013 GMT, May 12, 1970 and radar pictures from Wichita (left) and Kansas City, Missouri.

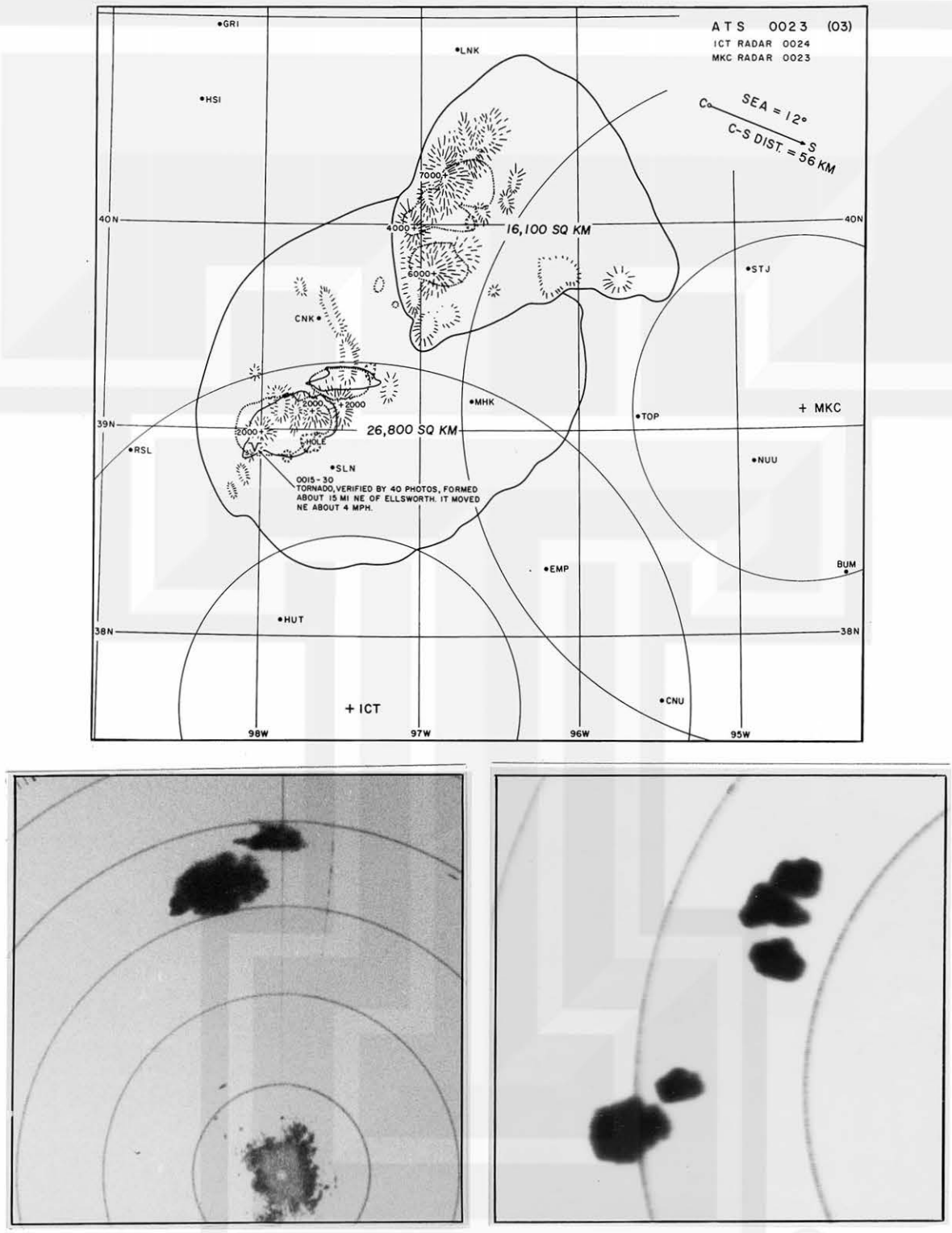

Fig. 13. ATS cloud patterns at 0023 GMT, May 12, 1970 and radar pictures from Wichita (left) and Kansas City, Missouri.

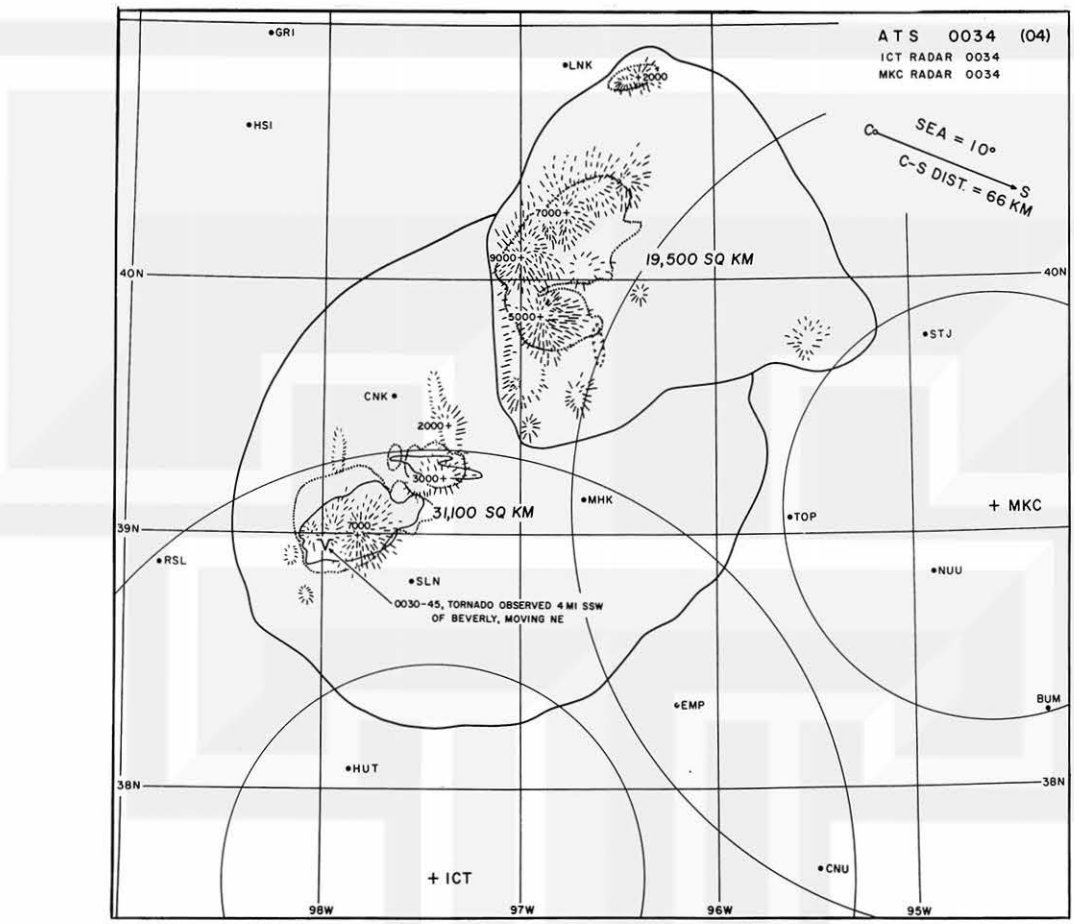

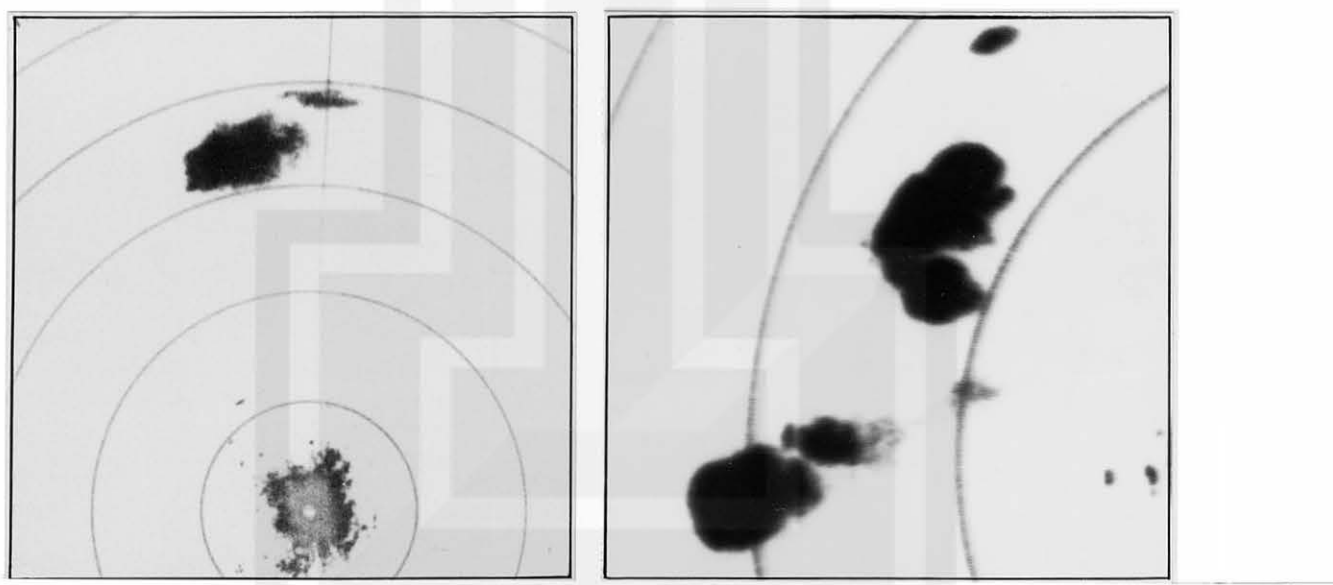

Fig. 14. ATS cloud patterns at 0034GMT, May 12, 1970 and radar pictures from Wichita (left) and Kansas City, Missouri.

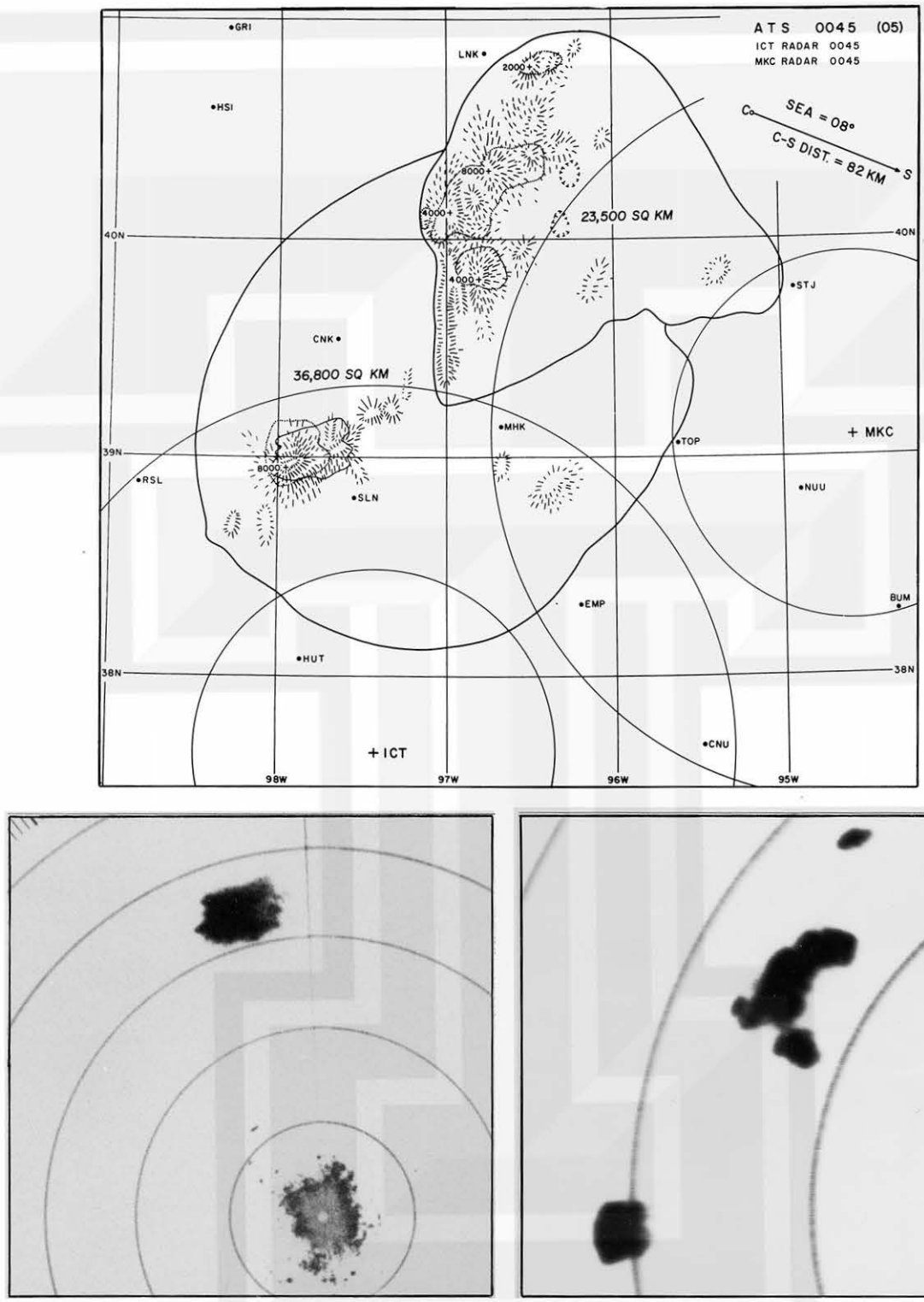

Fig. 15. ATS cloud patterns at 0045 GMT, May 12, 1970 and radar pictures from Wichita (left) and Kansas City, Missouri.

Followed by a funnel aloft observation, between 0015 and 0025 a slow-moving tornado was verified by 40 photos taken by Kansas State patrolmen. The tornado spawned from the small echo which had grown into a large intense echo as shown in 0023 chart. Although the echo was extensive, the cloud tops over the echo areas were rather flat, showing no distinct shadow features.

At 0034, a development of a shadow is seen over the tornado area, suggesting that an overshooting top started increasing its height above the anvil top. The major tornado disappeared by 0030 while a small one was sighted 4 miles south-southwest of Beverly.

3. TORNADO OCCURRENCES IN RELATION TO ANVIL GROWTH AND CLOUD-TOP HEIGHTS

The foregoing evidence shows that tornado occurrences are related to the heights of the overshooting tops located in the vicinity of the tornadoes. For further investigation of the relationship between tornado occurrences and the cloud-top

Table 1. Anvil areas and overshooting heights of CB near Salina, Kansas, May 11-12, 1970. The edge of the anvil was estimated from the shadow to be 42,000 ft MSL. The anvil-top height in the vicinity of overshooting tops is 2 to 3000 ft higher than the anvil edge.

Time (Z)	Anvil Areas in sq. km	Overshooting Heights in ft.
2244	1,100 + 900 = 2,000	
2256	1,900 + 1,700 = 3,600	
2307	3,800 + 2,000 = 5,800	7000 ft
2318	5,900 + 2,800 = 8,700	*5000, *3000
2329	8,700 + 3,500 = 12,200	6000, 5000
2340	12,000 + 5,300 = 15,300	6000, 5000, 5000, 3000
2351	15,400 + 7,800 = 23,200	7000, 4000, 3000
0002	18,700 + 10,500 = 29,200	9000, 7000, 4000, 3000
0013	21,700 + 13,900 = 35,600	9000, 4000, 3000, 2000, 2000
0023	26,800 + 16,100 = 42,900	7000, 6000, 4000, *2000, 2000, 2000
0034	31,100 + 19,500 = 50,600	9000, 7000, *7000, 5000, 3000, 2000
0045	36,800 + 23,500 = 60,300	8000, 8000, 4000, 4000, 4000, 2000

*within 15 miles from tornado

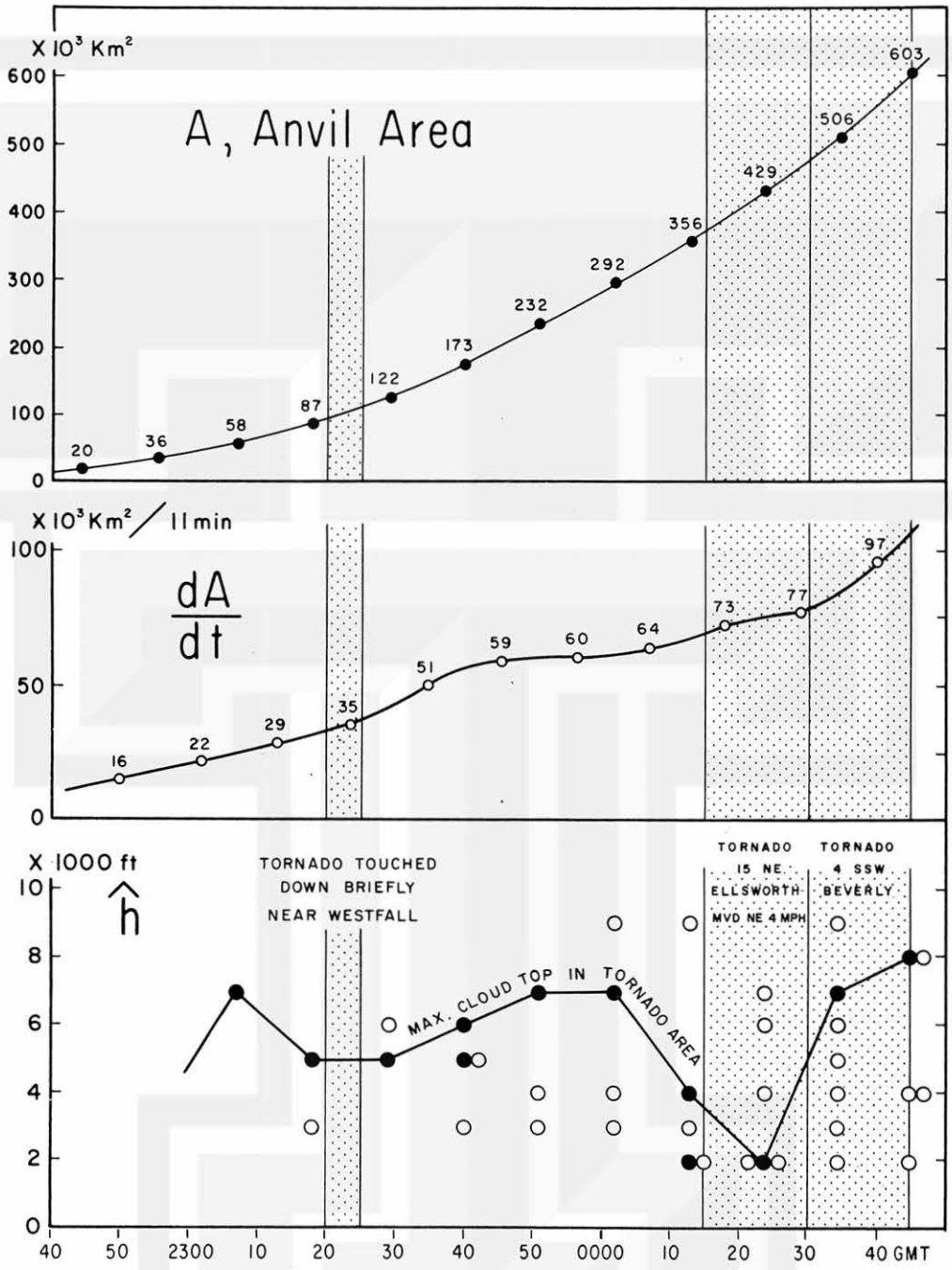

Fig. 16. Anvil area, its growth rate and the heights of overshooting tops in relation to tornado occurrences.

heights as well as the growth rate of anvil boundaries, Table 1 was compiled.

To show the relationship between the tornado occurrences and the anvil growth, the areas of two anvils combined were plotted in Fig. 16. The times of tornadoes are stippled. It is seen that the areal growth of the anvil is almost exponential with time, suggesting strongly that the combination of the rapid growth

and the increase in the number of convective cells inside the anvil contributed to this exponential growth.

When the rate of growth or the time derivative of anvil areas are compared with the tornado times, as shown in the middle diagram, there appears to be a tendency that tornadoes either weaken or die out when dA/dt increases. This evidence, which is opposite from what one would expect, coincides with Purdom's (1971) finding that tornado occurrences take place when anvil growth rate decreases. He concluded that the pause in anvil growth and tornado occurrences are correlated.

Shown in the bottom diagram in Fig. 16 is the time variation of the heights of overshooting tops above their environmental anvil. The basic data appear in Table 1 as well as in Figs. 4 through 15. Since three tornadoes spawned from this anvil complex were within a circle of 15 miles in diameter, all cloud-top heights within this circle were painted black. The diagram, thus obtained, clearly shows that the highest ones did not produce tornadoes, instead, tornadoes developed when nearby cloud-top height decreased. This is against the common belief that tornadoes are likely to spawn from vigorous thunderstorms reaching very high altitude. If we, for instance, compile statistics of tornado probability against the cloud-top height, the result would indicate that tornado- and non-tornado producers cannot be distinguished simply as a function of the height of cloud tops penetrating several thousand feet above the tropopause.

It should be noted that Bonner and Kemper's (1971) tornado probability as a function of echo-top heights (see Figs. 17 and 18) in three regions of the U. S. reveals that tornado probability does not increase significantly with echo-top height while hail probability increases almost exponentially with the height. Their results thus suggest that the echo-top height can be used as a primary hail predictor, while tornado occurrences are not too sensitive to the echo-top height.

4. CLOUD-TOP TOPOGRAPHY

The foregoing evidence suggests strongly that the mapping of cloud-top topography by all possible means is of vital importance in learning the overshooting mechanisms related apparently to the occurrences of tornadoes. Basic methods of cloud-top mapping are:

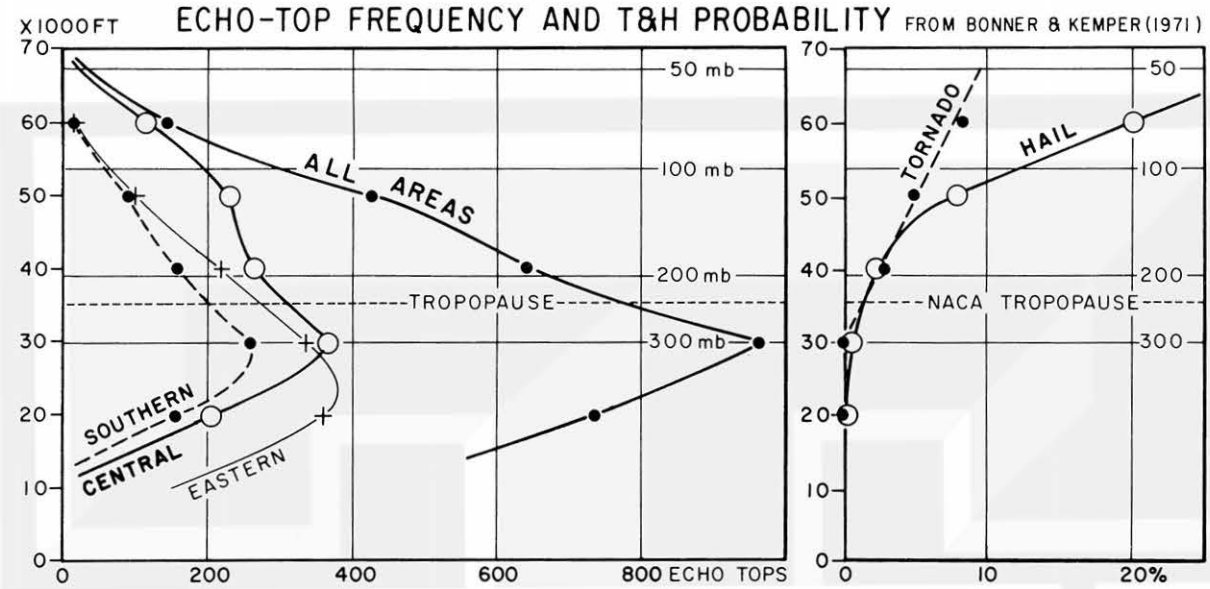

Fig. 17. Echo-top frequency and tornado and hail probability in three U. S. areas. After Bonner and Kemper (1971).

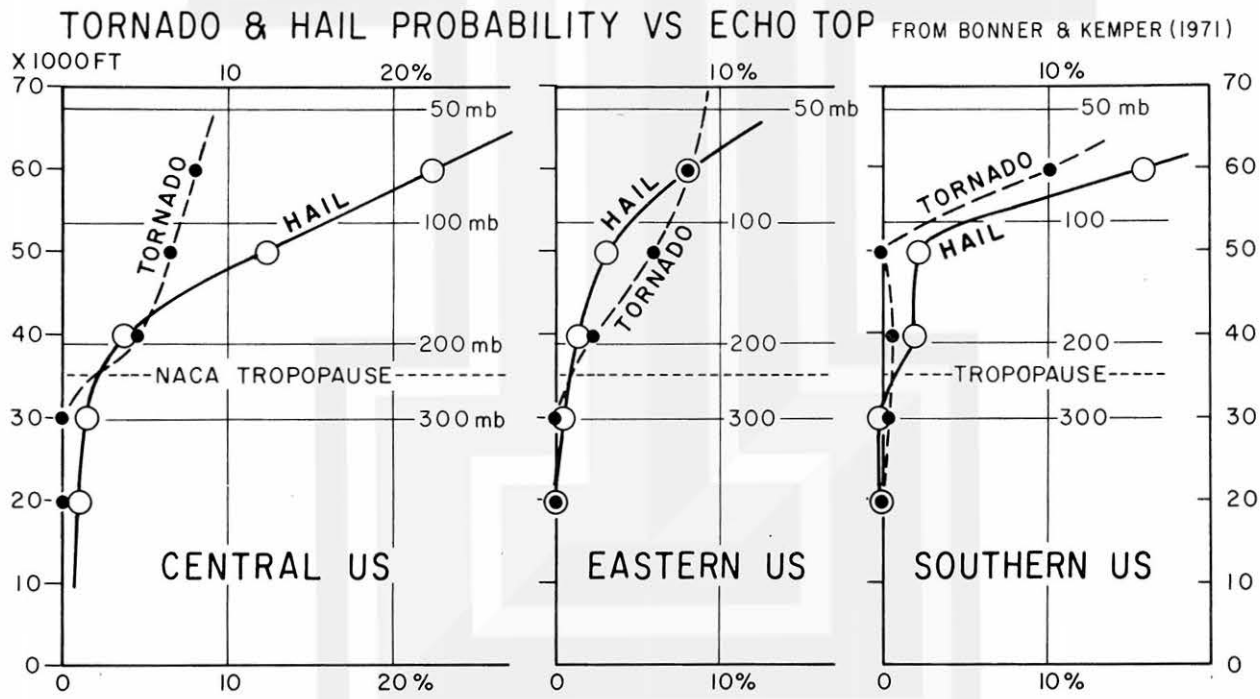

Fig. 18. Breakdown of tornado and hail probability in three U. S. areas. After Bonner and Kemper (1971).

(1) Stereoscopic Method

As demonstrated by Lee (1971) and others, successive pictures taken by RB-57 or U-2 aircraft can be used as stereopair photographs under the assumption that clouds in pair pictures do not move or change during the short time between two pictures. Shenk and Holub's (1971) cloud-top mapping from a stereo-pair Apollo 6 pictures paved a way to map large cloud areas which cannot be photographed by a high-flying airplane.

(2) Lunar Mapping Technique

Single-image photogrammetry has been used in mapping lunar-surface relief in which the camera and the sun are considered to be two separate observers looking at a given point on the moon from two different directions. The cloud-to-shadow relationships can thus be used to determine the heights of the objects above the shadow points.

(3) IR Mapping of Cloud-top Temperature

If we know the cloud-top temperature as a function of the cloud-top height, measured equivalent blackbody temperatures from either satellite or aircraft can be converted into the cloud-top height.

(4) RHI and/or PPI determination of Echo Heights

Although the top of radar echoes does not coincide with the cloud top, it is feasible to estimate the patterns of cloud-top topography over the overshooting area by means of RHI and/or spiral PPI scans which will permit us to determine the echo-top topography rather than the cloud-top topograhy.

There are other methods such as stereo measurement from ground-base cameras which are useful to determine the time variation of the cloud tops of unobstructed distant clouds. In order to obtain synoptic views of ever-changing cloud tops, however, discussion in this paper is limited to the mapping of three-dimensional features of cloud-top relief.

Presented in Fig. 19 is an example of 1000 ft relief contours of the Salina cloud in Fig. 3, the third picture from the last. The location of the tornado near 39N and 98W is not associated with high overshooting tops. There are three tall tops identified as D, E, and F which are located some 75 miles to the northeast of the tornado. No tornadoes were reported in the vicinity of these tops.

Although the relationship between the equivalent blackbody temperatures and overshooting tops is not known at the present time, an assumption of dry adiabatic processes inside the protrusion implies that overshooting tops are colder than surrounding anvil tops. Fig. 20 shows the distribution of equivalent blackbody temperatures measured by a down-looking IR sensor on board an Air Force U2 aircraft. The author in a DC-6B research aircraft determined the extent of a thick anvil while flying just below the anvil base. The statistics shown in the lower right corner of the figure reveal the temperature frequencies measured while flying over the regions of weak and moderate echoes photographed by the Oklahoma City radar. The mean IR temperatures over anvil being -46° , over weak echoes, -48° , and over moderate echoes, -50° suggest a significant decrease in the equivalent blackbody temperatures from overall anvil to moderate echo areas. If a scanning radiometer were used to depict patterns of IR temperature along a band both sides of the aircraft track, overshooting tops are likely to appear as cold dome tops.

5. LABORATORY SIMULATION OF TORNADO FORMATION

In an attempt to learn more about the mechanism of the tornado formation at the time of "the pause in anvil growth by Purdom", "insignificant height of cloud tops by Lee", and "the subsiding phase of the cloud-top height by Fujita", the author constructed a simple laboratory model shown in Fig. 21.

The model is characterized by (a) holes which can be opened or closed to induce a cloud-scale updraft, (b) cups rotated by six concentric shafts which are driven from above to generate Rankine vortex with varying core diameters and speeds, (c) the combined system which can travel through a distance of 15 ft at four speeds, and (d) the ground surface which may move up and down to change the depth of the atmosphere below the rotating cups. Dry-ice fog has been used as the tracer to make vortices visible. Note that a dark tube surrounded by dry-ice fog

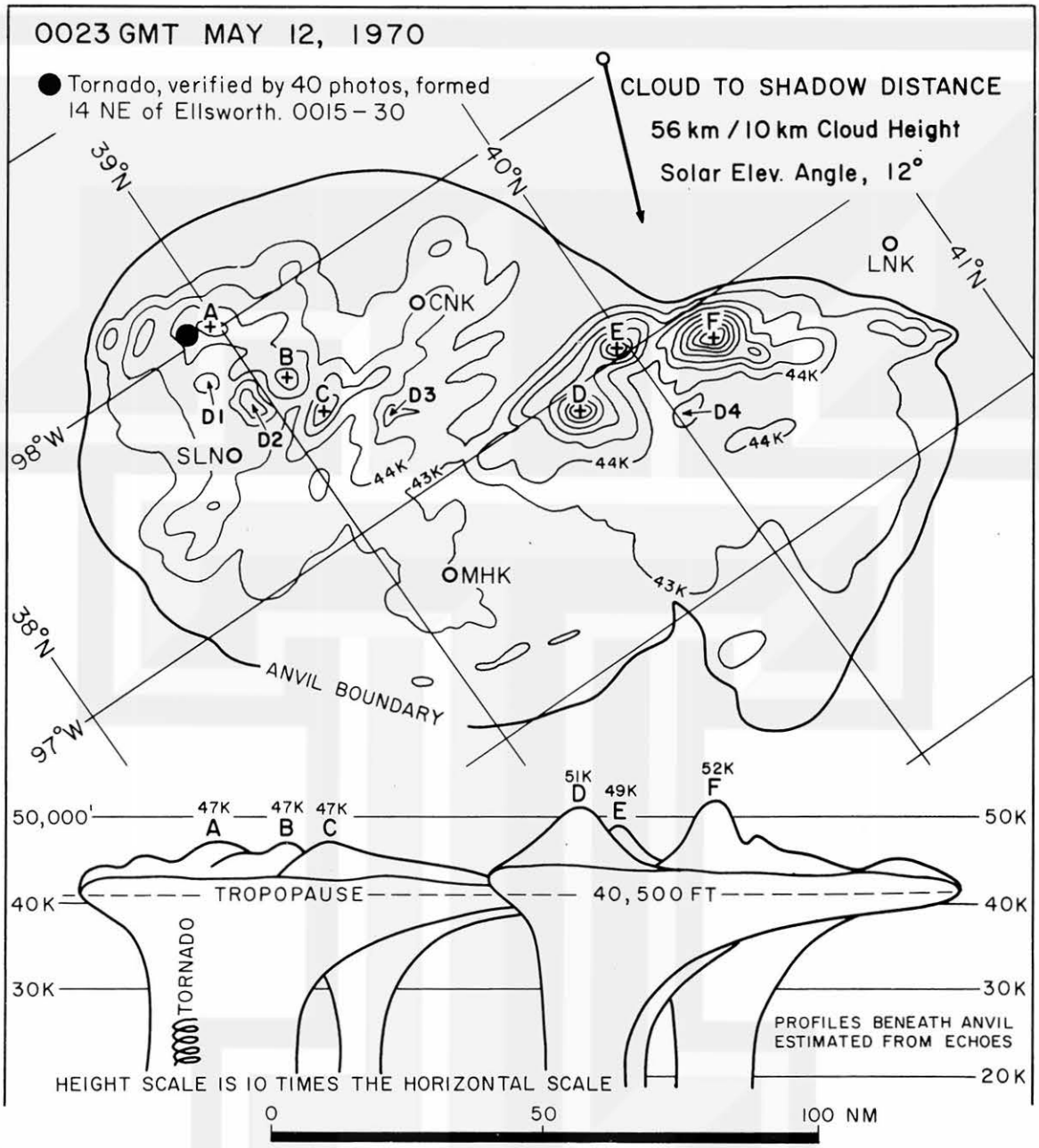

Fig. 19. Anvil-top topography of Salina cloud when a tornado verified by 40 photos formed near Ellsworth. The anvil top was contoured for every 1000 ft. using the cloud-shadow relationship. Contours designated by arrows and letter D are shallow depressions of the anvil top.

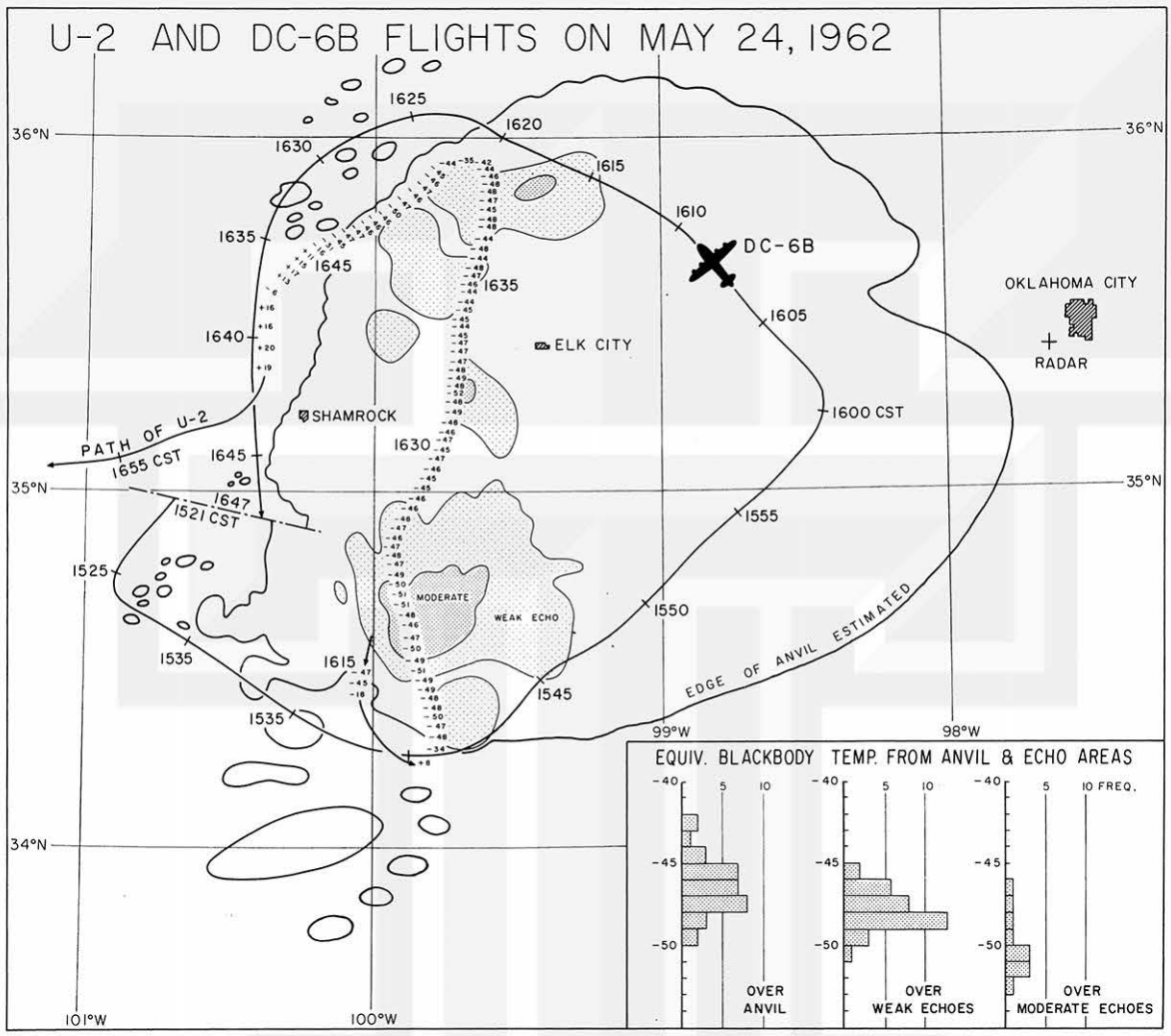

Fig. 20. Equivalent blackbody temperatures measured by a down-looking radiometer on board a U-2. Statistical analysis shows that the tops of convective regions are colder than overall anvil area.

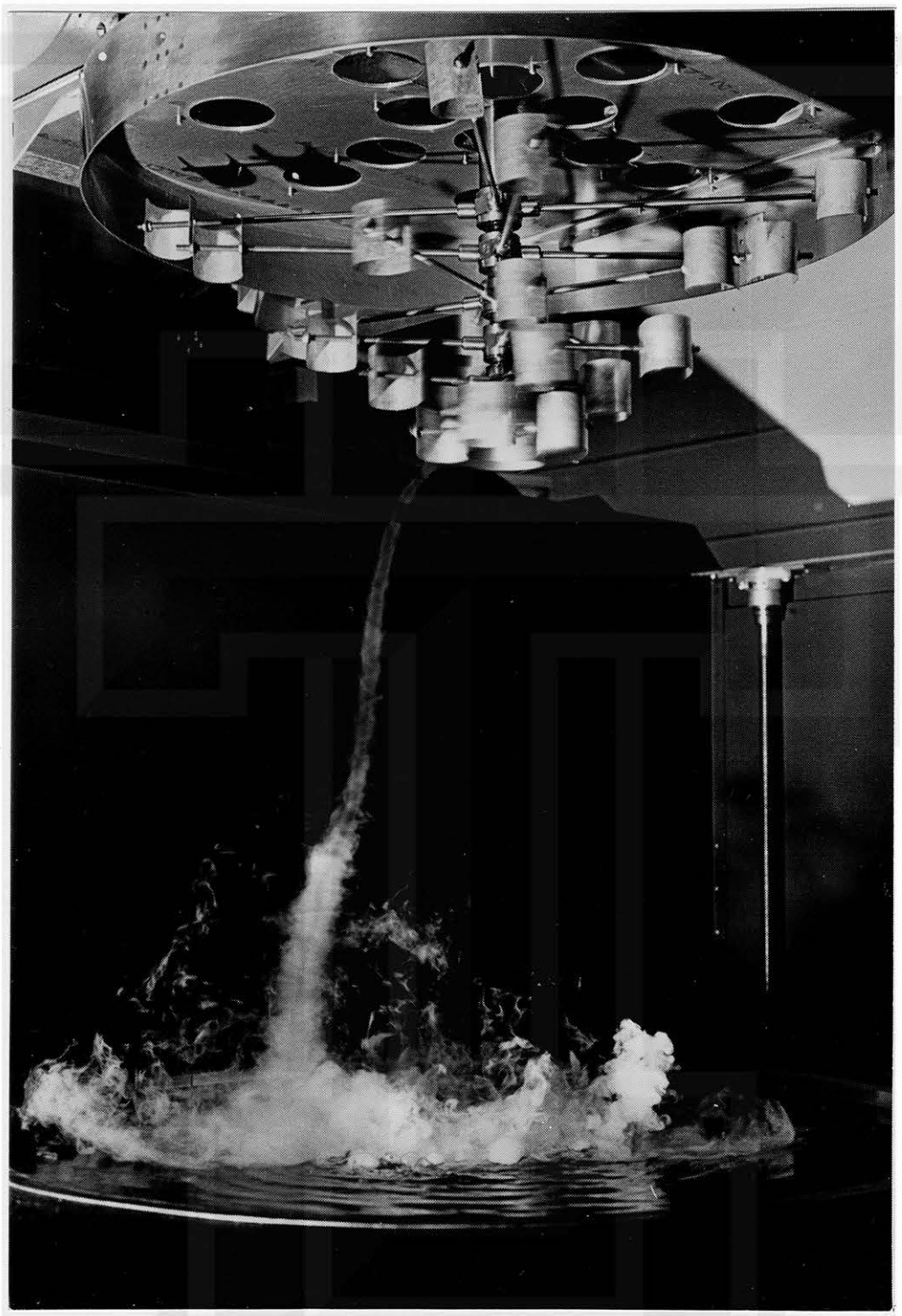

Fig. 21. Laboratory simulation of tornado producing thunderstorms characterized by both rotation and updraft. Note that the horizontal dimensions of surface vortex are at least one order of magnitude smaller than the cloud scale rotation field.

extends from the surface all the way to the outer edge of the Rankine core ending at the edge of the innermost cup.

Repeated simulation resulted in a matrix of very interesting pictures (see Fig. 22). As indicated by arrows the cloud-scale rotation increases 0 to 8 units so does the updraft 0 to 2 in four steps. In this experiment, the updraft was added only around the core rotation, thus closing the innermost updraft holes, because the natural cloud system is characterized by a rotating updraft around the rotation core in which air could move either up or downward rather slowly.

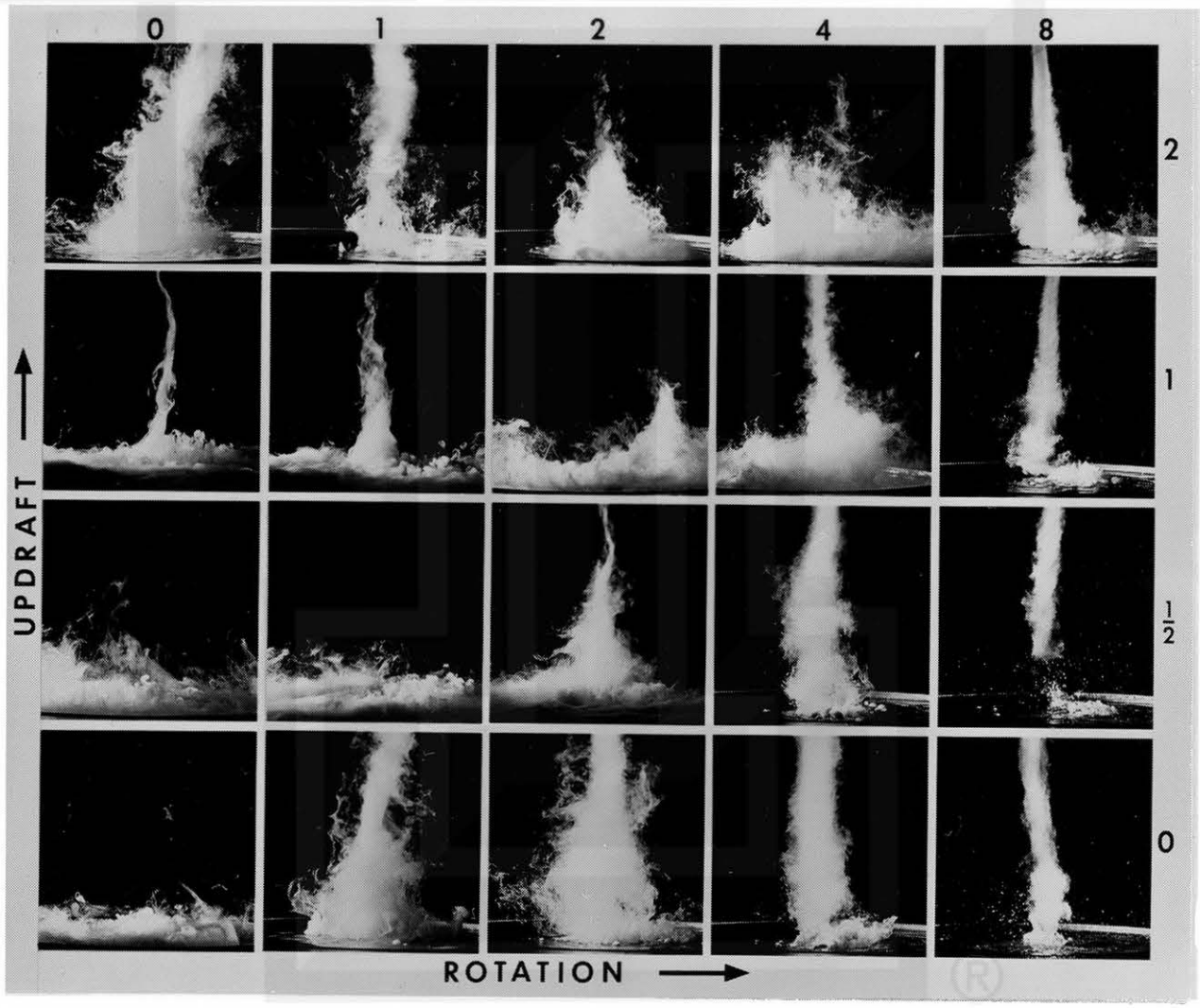

Fig. 22. A matrix of simulated tornado pictures obtained by changing both rotation and updraft into 20 combinations.

As expected the simulated tornado intensifies when the rotation increases, thus initiating spray of water seen as bright dots. Updraft without rotation definitely induces a vortex, the intensity of which increases with the updraft intensity.

A very strange thing, however, is the reduction of the vortex intensity when both rotation and updraft are added together. Examination of Fig. 22 will reveal that there are only very weak or no vortices in these pictures along a diagonal line extending lower left to upper right. This would mean that updraft and rotation do not cooperate together in inducing strong vortices on the ground, despite the fact that each of these parameters while acting independent of each other does produce tornadoes.

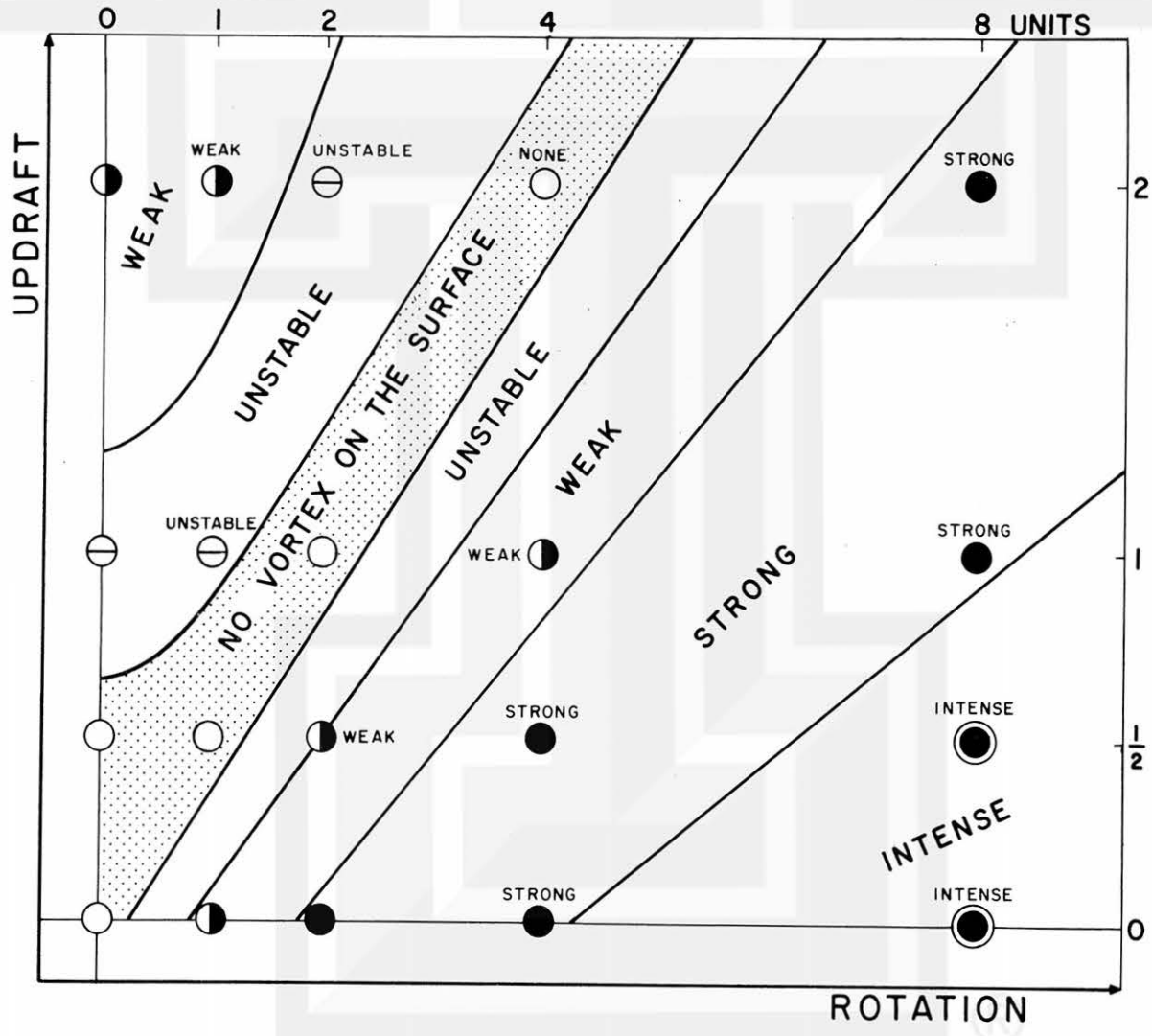

Fig. 23. A diagram showing the domains of varying vortex intensities. A domain of no vortex extends from the origin toward the upper right.

Shown in Fig. 23 is the summary of the picture matrix. Note the existence of a stippled area corresponding to the domain of no vortex on the surface. As we move to the lower right, tornado intensity increases from unstable, weak, strong to intense. These may be identified as being the "rotation-induced tornadoes". The domain of unstable to weak tornado in the upper left portion of the diagram may be called the "updraft-induced tornadoes". The term "tornadoes" was used with the understanding that they are laboratory simulated vortices one order of magnitude smaller than the simulated cloud aloft.

Without further development of Doppler radars it is not feasible to assess the degree of rotation and updraft of various thunderstorms which may or may not be tornado producers. The laboratory simulation, however, shows positively that thunderstorms with weak rotational characteristics do not produce tornadoes because they are characterized by medium to strong updraft as well. Rotating thunderstorms such as might be identified as hook-echo storms are very likely to produce strong tornadoes in their pausing or slowing down phase of rotating updraft. If the updraft pulsates with a certain period we may expect to find the periodic occurrences of family tornadoes rather regularly. Both Fujita (1963) and Darkow (1971) pointed out the existence of a 45 min mean occurrence interval of family tornadoes.

6. CONCLUSIONS

Detailed analysis of ATS picture sequence of anvil clouds near Salina, Kansas revealed that tornadoes occur during the decreasing to pausing stage of the parent cloud top, suggesting that excessive updraft could be acting as a damper on the formation of tornadoes. A laboratory simulation of parent cloud and tornado indicated also that an excessive updraft added to a rotating cloud tends to kill the tornado.

It is concluded, therefore, that the determination of the time variation of updraft is of vital importance in understanding the nature of thunderstorm updrafts. As a first step of this research it is essential to observe the time variation of both height and shape of the cloud tops overshooting beyond the overall anvil level.

Such an objective can be achieved by performing a combined effort of

i) IR measurements of cloud-top temperature from aircraft.

ii) Cloud photography from overflying aircraft.

iii) Horizontal photography from aircraft at anvil level.

iv) Radar photographs, RHI and/or spiral PPI, and Doppler.

The data can be analyzed to determine the nature of overshooting in relation to its time and space variations. The final goal is, of course, to monitor the anvil tops from geostationary satellites for the severe storm watch and subsequent warning purposes. Nevertheless, the basic information for satellite design criteria must be obtained and justified based on these proposed measurements.

References

Bonner, W. D. and J. E. Kemper (1971): Broad-scale Relations between Radar and Severe Weather Reports. Reprint, 7th Conference on Severe Local Storms, Kansas City, Mo., Oct. 1971, pp. 140-147.

Darkow, G. L. (1971): Periodic Tornado Production by Long-lived Parent Thunderstorms. Preprint of 7th Severe Local Storms Conference, Kansas City, Mo., Oct. 1971, pp. 214-217.

Fujita, T. T. (1963): Analytical Mesometeorology: A Review. Meteor. Monograph, 5, No. 27, AMS, pp. 77-125.

Fujita, T. T. and J. Arnold (1963): Preliminary Result of Analysis of the Cumulonimbus Cloud of April 21, 1961. SMRP Research Paper 16.

Lee, J. T. (1971): Aerial Survey of Tornado-producing Thunderstorms. Preprint, 7th Conference on Severe Local Storms, Kansas City, Mo., October 1971, pp. 49-53.

Purdom, J. F. W. (1971): Satellite Imagery and Severe Weather Warnings. Preprint of Seventh Conference on Severe Local Storms, Kansas City, Mo., pp. 120-127.

Remick, J. H. (1971): Radar Reflectivity Profile of Individual Cells in a Persistent Multicellular Alberta Hailstorm. Preprint, 7th Conference on Severe Local Storms, Kansas City, October 1971, pp. 63-70.

Shenk, W. E. and R. Holub (1971): An Example of Detailed Cloud Contouring from Apollo 6 Photography. Bull. of AMS, 52, cover and p. 238.

MESOMETEOROLOGY PROJECT - - - RESEARCH PAPERS

(Continued from front cover)

42.* A Study of Factors Contributing to Dissipation of Energy in a Developing Cumulonimbus - Rodger A. Brown and Tetsuya Fujita

43. A Program for Computer Gridding of Satellite Photographs for Mesoscale Research - William D. Bonner

44. Comparison of Grassland Surface Temperatures Measured by TIROS VII and Airborne Radiometers under Clear Sky and Cirriform Cloud Conditions - Ronald M. Reap

45. Death Valley Temperature Analysis Utilizing Nimbus I Infrared Data and Ground-Based Measurements - Ronald M. Reap and Tetsuya Fujita

46. On the "Thunderstorm-High Controversy" - Rodger A. Brown

47. Application of Precise Fujita Method on Nimbus I Photo Gridding - Lt. Cmd. Ruben Nasta

48. A Proposed Method of Estimating Cloud-top Temperature, Cloud Cover, and Emissivity and Whiteness of Clouds from Short- and Long-wave Radiation Data Obtained by TIROS Scanning Radiometers - T. Fujita and H. Grandoso

49. Aerial Survey of the Palm Sunday Tornadoes of April 11, 1965 - Tetsuya Fujita

50. Early Stage of Tornado Development as Revealed by Satellite Photographs - Tetsuya Fujita

51. Features and Motions of Radar Echoes on Palm Sunday, 1965 - D. L. Bradbury and T. Fujita

52. Stability and Differential Advection Associated with Tornado Development - Tetsuya Fujita and Dorothy L. Bradbury

53. Estimated Wind Speeds of the Palm Sunday Tornadoes - Tetsuya Fujita

54. On the Determination of Exchange Coefficients: Part II - Rotating and Nonrotating Convective Currents - Rodger A. Brown

55. Satellite Meteorological Study of Evaporation and Cloud Formation over the Western Pacific under the Influence of the Winter Monsoon - K. Tsuchiya and T. Fujita

56. A Proposed Mechanism of Snowstorm Mesojet over Japan under the Influence of the Winter Monsoon - T. Fujita and K. Tsuchiya

57. Some Effects of Lake Michigan upon Squall Lines and Summertime Convection - Walter A. Lyons

58. Angular Dependence of Reflection from Stratiform Clouds as Measured by TIROS IV Scanning Radiometers - A. Rabbe

59. Use of Wet-beam Doppler Winds in the Determination of the Vertical Velocity of Raindrops inside Hurricane Rainbands - T. Fujita, P. Black and A. Loesch

60. A Model of Typhoons Accompanied by Inner and Outer Rainbands - Tetsuya Fujita, Tatsuo Izawa,, Kazuo Watanabe and Ichiro Imai

61. Three-Dimensional Growth Characteristics of an Orographic Thunderstorm System - Rodger A. Brown

62. Split of a Thunderstorm into Anticyclonic and Cyclonic Storms and their Motion as Determined from Numerical Model Experiments - Tetsuya Fujita and Hector Grandoso

63. Preliminary Investigation of Peripheral Subsidence Associated with Hurricane Outflow - Ronald M. Reap

64. The Time Change of Cloud Features in Hurricane Anna, 1961, from the Easterly Wave Stage to Hurricane Dissipation - James E. Arnold

65. Easterly Wave Activity over Africa and in the Atlantic with a Note on the Intertropical Convergence Zone during Early July 1961 - James E. Arnold

66. Mesoscale Motions in Oceanic Stratus as Revealed by Satellite Data - Walter A. Lyons and Tetsuya Fujita

67. Mesoscale Aspects of Orographic Influences on Flow and Precipitation Patterns - Tetsuya Fujita

68. A Mesometeorological Study of a Subtropical Mesocyclone -Hidetoshi Arakawa, Kazuo Watanabe, Kiyoshi Tsuchiya and Tetsuya Fujita

69. Estimation of Tornado Wind Speed from Characteristic Ground Marks - Tetsuya Fujita, Dorothy L. Bradbury and Peter G. Black

70. Computation of Height and Velocity of Clouds from Dual, Whole-Sky, Time-Lapse Picture Sequences - Dorothy L. Bradbury and Tetsuya Fujita

71. A Study of Mesoscale Cloud Motions Computed from ATS-I and Terrestrial Photographs - Tetsuya Fujita, Dorothy L. Bradbury, Clifford Murino and Louis Hull

72. Aerial Measurement of Radiation Temperatures over Mt. Fuji and Tokyo Areas and Their Application to the Determination of Ground- and Water-Surface Temperatures - Tetsuya Fujita, Gisela Baralt and Kiyoshi Tsuchiya

73. Angular Dependence of Reflected Solar Radiation from Sahara Measured by TIROS VII in a Torquing Maneuver - Rene Mendez.

74. The Control of Summertime Cumuli and Thunderstorms by Lake Michigan During Non-Lake Breeze Conditions - Walter A. Lyons and John W. Wilson

75. Heavy Snow in the Chicago Area as Revealed by Satellite Pictures - James Bunting and Donna Lamb

76. A Model of Typhoons with Outflow and Subsidence Layers - Tatsuo Izawa

* out of print

(continued on outside back cover)

SATELLITE AND MESOMETEOROLOGY RESEARCH PROJECT --- PAPERS
(Continued from inside back cover)

77. Yaw Corrections for Accurate Gridding of Nimbus HRIR Data - Roland A. Madden

78. Formation and Structure of Equatorial Anticyclones Caused by Large-Scale Cross Equatorial Flows Determined by ATS I Photographs - Tetsuya T. Fujita and Kazuo Watanabe and Tatsuo Izawa.

79. Determination of Mass Outflow from a Thunderstorm Complex Using ATS III Pictures - T. T. Fujita and D. L. Bradbury.

80. Development of a Dry Line as Shown by ATS Cloud Photography and Verified by Radar and Conventional Aerological Data - Dorothy L. Bradbury.

81. Dynamical Analysis of Outflow from Tornado-Producing Thunderstorms as Revealed by ATS III Pictures - K. Ninomiya.

82. ** Computation of Cloud Heights from Shadow Positions through Single Image Photogrammetry of Apollo Pictures - T. T. Fujita.

83. Aircraft, Spacecraft, Satellite and Radar Observations of Hurricane Gladys, 1968 - R. Cecil Gentry, Tetsuya T. Fujita and Robert C. Sheets.

84. Basic Problems on Cloud Identification Related to the Design of SMS-GOES Spin Scan Radiometers - Tetsuya T. Fujita.

85. Mesoscale Modification of Synoptic Situations over the Area of Thunderstorms' Development as Revealed by ATS III and Aerological Data - K. Ninomiya.

86. Palm Sunday Tornadoes of April 11, 1965 - T. T. Fujita, Dorothy L. Bradbury and C. F. Van Thullenar (Reprint from Mon. Wea. Rev., 98, 29-69, 1970).

87. Patterns of Equivalent Blackbody Temperature and Reflectance of Model Clouds Computed by Changing Radiometer's Field of View - Jaime J. Tecson.

88. Lubbock Tornadoes of 11 May 1970 - Tetsuya Theodore Fujita.

89. Estimate of Areal Probability of Tornadoes from Inflationary Reporting of Their Frequencies - Tetsuya T. Fujita.

90. Application of ATS III Photographs for Determination of Dust and Cloud Velocities Over Northern Tropical Atlantic - Tetsuya T. Fujita.

91. A Proposed Characterization of Tornadoes and Hurricanes by Area and Intensity - Tetsuya T. Fujita.

92. Estimate of Maximum Wind Speeds of Tornadoes in Three Northwestern States - T. Theodore Fujita.

93. In- and Outflow Field of Hurricane Debbie as Revealed by Echo and Cloud Velocities from Airborne Radar and ATS-III Pictures - T. T. Fujita and P. G. Black (Reprinted from preprint of Radar Meteorology Conference, November 17-20, 1970, Tucson, Arizona).

94. ** Characterization of 1965 Tornadoes by their Area and Intensity - Jaime J. Tecson.

95. * Computation of Height and Velocity of Clouds over Barbados from a Whole-Sky Camera Network - Richard D. Lyons.

96. The Filling over Land of Hurricane Camille, August 17-18, 1969 - Dorothy L. Bradbury.